July/August 2023 | mwrf.com

Microwaves&RF®

Take a BUILDING-BLOCK APPROACH to RF System Design

PULSAR
MICROWAVE CORPORATION

DC to 85 GHZ

HIGH PERFORMANCE COMPONENTS

Directional Couplers, to 60 GHz
Single and Dual
High Power, to 2500 watts

Power Dividers, to 70 GHz
2-32 Way

Bias Tees, to 85 GHz
From 30 KHz

Hybrids, to 40 GHz
90° & 180°

CUSTOMIZATION AVAILABLE, QUOTES IN 24 HOURS.
www.pulsarmicrowave.com

48 Industrial West, Clifton, NJ 07012 | email: sales@pulsarmicrowave.com
Tel: 973-779-6262 • Fax: 973-779-2727

RoHS Compliant
ISO 9001:2008 Certified
60/40 Solder Also Available

CONTENTS

July/August 2023 | VOLUME 62, ISSUE 4

FEATURES

DEPARTMENTS

Cover image: vittaya25 1354880452 | iStock / Getty Images Plus

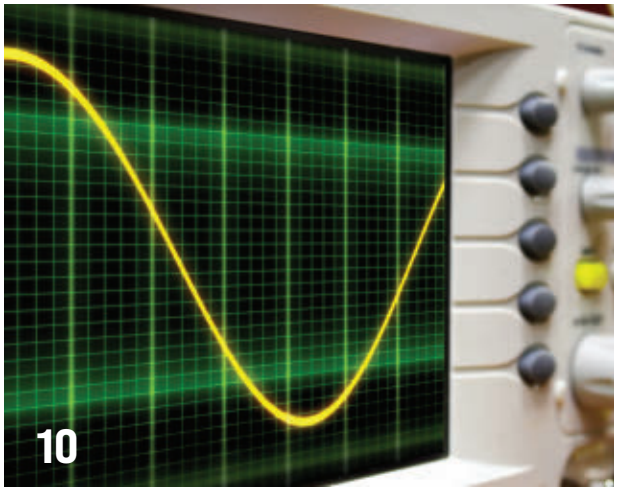

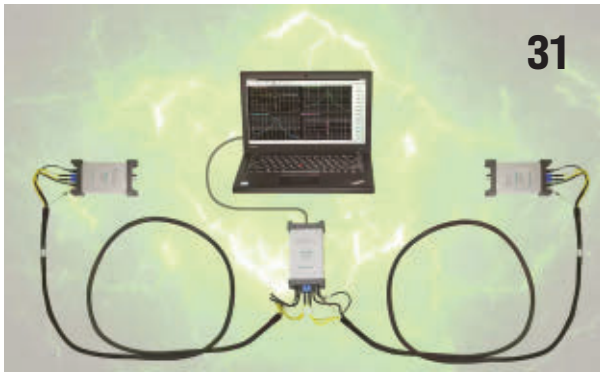

DAVID MALINIAK, Senior Editor

IMS 2023
in the Rearview Mirror

At a reinvigorated International Microwave Symposium, the industry flexes its muscle and points to a bright future.

Sergiy Palamarchuk 109336976 | Dreamstime.com

FOR A FEW YEARS NOW, the International Microwave Symposium (IMS), like virtually all in-person industry events, had been in the doldrums. Despite its reputation as "the flagship event dedicated to all things microwave," attendees and vendors alike were hedging their bets and hanging back, either scaling down their participation or just not showing up at all. The lingering effects of the COVID-19 pandemic, combined with our broad societal acceptance of working remotely and teleconferencing, served to throw a blanket over IMS.

Well, with IMS 2023 having recently concluded at the San Diego Convention Center, I can say without hesitation that those doldrums have passed. In fact, IMS 2023 was a blast! The exhibit floor, conference sessions, workshops, and social events were all extremely busy. As an editor whose days at IMS are full of non-stop meetings with industry experts, navigating the crowded aisles of the exhibit hall was challenging. Apologies to those who waited patiently for me to reach your booths.

Fortunately, all of the breathless running around was rewarded with a broad overview of the industry that you can get only at IMS. Here are some snapshots of highlights with links to our full coverage:

Analog Devices's Apollo MxFE front-end platform

Among the most impressive IMS launches was ADI's software-defined, direct RF-sampling, wideband, mixed-signal front-end platform. With Apollo MxFE, ADI has in its sights the future of phased-array radar, signals intelligence, industrial IoT, advanced test and measurement, mil/aero, and more. We're talking about the industry's first integrated radio that covers the 6G bands from 7 to 15 GHz with instantaneous bandwidths up to 10 GHz.

Tektronix's SignalVu-PC vector-signal-analysis software

Oscilloscopes have long since cemented their places on RF/mmWave designers' testbenches, but they continue to add functionality by way of new application-specific software. To that end, Tektronix now offers multichannel vector-signal-analysis capabilities in its 5 and 6 MSO Series platforms. The software endows the oscilloscopes with the functionality of a vector signal analyzer, pulse analyzer, WiGig or WLAN tester, and spectrum analyzer—all coupled with the advanced triggers of a digital scope.

Microchip Technology's chip-scale atomic clock

Timing is everything in life, and even more so in digital circuits. Microchip came to IMS with an interesting demo of its SA65 chip-scale atomic clock, which the company says is the world's lowest-power chip in its class (<120 mW). The device delivers short-term stability (Allan Deviation) of 3.0×10^{-10} at $\tau = 1$ s from −40 to +80°C. The SA65 has all you need to quantify oscillators.

Those are just a handful of interesting launches and demos we saw at IMS 2023. There's lots more where that came from in our online issue with full IMS 2023 coverage, with more being added as I write. If you couldn't get to San Diego, I hope our efforts provide you with at least a flavor of what the show was like. ■

dmaliniak@endeavorb2b.com

EDITORIAL ADVISORY BOARD

AD INDEX

Microwaves&RF
mwrf.com

EDITORIAL

Group Content Director: Michelle Kopier
mkopier@endeavorb2b.com

Senior Content Editor: Bill Wong
bwong@endeavorb2b.com

Senior Editor: David Maliniak
dmaliniak@endeavorb2b.com

Managing Editor: Roger Engelke
rengelke@endeavorb2b.com

Editor-at-Large: Alix Paultre
apaultre@endeavorb2b.com

Senior Staff Writer: James Morra
jmorra@endeavorb2b.com

Technical Editor: Jack Browne,
jack.browne@citadeleng.com

ART & PRODUCTION

Group Design Director: Anthony Vitolo

Art Director: Jocelyn Hartzog

Production Manager: Brenda Wiley

Ad Services Manager: Deanna O'Byrne

AUDIENCE MARKETING

User Marketing Manager: Debbie Brady
dmbrady@endeavorb2b.com

Article Reprints:
reprints@endeavorb2b.com

LIST RENTAL

Smartreach Client Services Manager:
Mary Ralicki, mralicki@endeavorb2b.com

DIGITAL & MARKETING

VP Digital & Data Innovation: Ryan Malec

SALES

AL, AR, SOUTHERN CA, CO, FL, GA, HI, IA, ID, IL, IN, KS, KY, LA, MI, MN, MO, MS, MT, NC, ND, NE, OH, OK, SC, SD, TN, UT, VA, WI, WV, WY, CENTRAL CANADA:
Jamie Allen, jallen@endeavorb2b.com

AZ, NM, TX: Gregory Montgomery
gmontgomery@endeavorb2b.com

CT, DE, MA, MD, ME, NH, NJ, NY, PA, RI, VT, EASTERN CANADA:
Elizabeth Eldridge
eeldridge@endeavorb2b.com

AK, NORTHERN CA, NV, OR, WA, WESTERN CANADA, AUSTRIA, BELGIUM, FRANCE, GERMANY, LUXEMBURG, NETHERLANDS, PORTUGAL, SCANDINAVIA, SPAIN, SWITZERLAND, UNITED KINGDOM:
Stuart Bowen,
sbowen@endeavorb2b.com

ITALY: Diego Casiraghi,
diego@casiraghi-adv.com

PAN-ASIA: Helen Lai
helen@twoway-com.com

PAN-ASIA: Charles Liu
liu@twoway-com.com

ENDEAVOR BUSINESS MEDIA

ENDEAVOR BUSINESS MEDIA, LLC
30 Burton Hills Blvd., Suite 185.,
Nashville, TN 37215 | 800-547-7377

CEO: Chris Ferrell

President: June Griffin

CFO: Mark Zadell

COO: Patrick Rains

CRO: Reggie Lawrence

Chief Digital Officer: Jacquie Niemiec

Chief Administrative and Legal Officer: Tracy Kane

EVP, Design & Engineering Group: Tracy Smith

DESIGN & ENGINEERING GROUP
Electronic Design, Machine Design, Microwaves & RF, Power & Motion, SourceESB, Source Today, 3DX

Microwaves & RF Magazine ID Statement 2023:

Microwaves & RF, ISSN 2162-1411 online, is published 6 times a year (January/February, March/April, May/June, July/August, September/October, November/December) by Endeavor Business Media, LLC. 1233 Janesville Ave., Fort Atkinson, WI 53538.

POSTMASTER: Send address changes to Microwaves & RF, PO Box 3257, Northbrook, IL 60065-3257. **SUBSCRIPTIONS:** Publisher reserves the right to reject non-qualified subscriptions. Subscription prices: U.S. $68.75 per year; Canada/Mexico $81.25 per year; All other countries $93.75 per year. All subscriptions are payable in U.S. funds. Send subscription inquiries to Microwaves & RF, PO Box 3257, Northbrook, IL 60065-3257. Customer service can be reached toll-free at 877-382-9187 or at microwavesRF@omeda.com for magazine subscription assistance or questions.

Video ▸ Double-Pulse Tester Measures Wide-Bandgap Power Modules

The PD1550A from Keysight Technologies performs measurements of wide-bandgap semiconductor power modules, ensuring repeatable, reliable double-pulse test (DPT) results for the dynamic characterization of wide-bandgap (WBG) power modules. Features include probe compensation, offset adjustment, de-skewing, and common-mode noise rejection, with an innovative measurement topology and layout. **www.mwrf.com/21266932**

Video ▸ What's a QuarterBack Connector?

There's lots of applications for cable assemblies in which you want some extra assurance of mechanical retention. SV Microwave's latest offering, which it calls a QuarterBack connector, goes beyond a simple blind-mate SMP (or SMPM) interface to a bayonet-style connection. Giving the connector a quarter-turn upon mating engages a spring-loaded mechanism that locks the cable assembly in place. Unmating requires just a quarter-turn in the opposite direction and pulling out the blind-mate pin. **www.mwrf.com/21268472**

www.facebook.com/microwavesrf

linkedin.com/groups/3848060/profile

@MicrowavesRF

www.youtube.com/@engineeringtvEBM

Understanding Phase-Noise Measurement Techniques

Phase noise can be measured and analyzed either with traditional spectrum analyzers or dedicated phase-noise analyzers.
www.mwrf.com/21268395

Open RAN Radio-Unit Verification Speeds Design and Production

This development enables Open RAN radio unit and gNodeB vendors to accelerate design and production of Qualcomm QRU100 5G RAN Platform devices, and expands the portfolio of validated instruments and software solutions.
www.mwrf.com/21268388

11 Myths About Silicon Carbide

Looking to use silicon carbide (SiC) in your design? Make sure you don't get fooled by some of the myths surrounding this technology.
www.mwrf.com/21268292

Introducing the world's smallest high-frequency wirewound chip inductor!

Actual Size
(Tiny, isn't it?)

Once again, Coilcraft leads the way with another major size reduction in High-Q wirewound chip inductors

Measuring just 0.47 x 0.28 mm, with an ultra-low height of 0.35 mm, our new 016008C Series Ceramic Chip Inductors offer up to 40% higher Q than all thin film types: up to 62 at 2.4 GHz.

High Q helps minimize insertion loss in RF antenna impedance matching circuits, making the 016008C ideal for high-frequency applications such as cell phones, wearable devices, and LTE or 5G IoT networks.

The 016008C Series is available in 36 carefully selected inductance values ranging from 0.45 nH to 24 nH, with lower DCR than all thin film counterparts.

Find out why this small part is such a big deal. Download the datasheet and order your free samples today at **www.coilcraft.com.**

Coilcraft®

WWW.COILCRAFT.COM

Advanced Cable Tester Meets USB Type-C, HDMI 2.1 Requirements

This cost-effective tester provides fast test results and complete coverage of cable electrical signal integrity.

THE EXPLOSION IN connected devices isn't just putting pressure on wireless systems and infrastructures—it's placed significant speed and performance demands on wiring and cabling as well.

The latest generation of cables must transfer signals 2X to 4X faster than legacy solutions, plus deliver much more power. To meet the latest stringent design and production requirements, these wires and cables need new kinds of testing to ensure quality data transmission with zero defects.

Poor cables not only fail the new market requirements for high-speed performance, but cable manufacturers that either inadequately test high-speed cables or resort to custom-built test-equipment racks waste money in a costly and slow process that doesn't meet the demand.

Automated Cable Tester

To address these issues, Teledyne LeCroy developed an automated cable tester *(see image above)* to meet the production test requirements of USB Type-C, HDMI 2.1, and other advanced cables at transfer rates up to 48 Gb/s. The automated tester quickly performs all required electrical and signal-integrity tests, with low up-front capital equipment and operating costs.

The RapidWave4000's USB Type-C cable ports support data transfer via USB4, USB 3.2, DisplayPort 2.0, Thunderbolt 3, and Thunderbolt 4 standards. Meanwhile, its Production Module rapidly performs production tests such as continuity, dc resistance (DCR), quiescent current and E-marker readout (for USB Type-C cables), and signal-integrity insertion-loss testing. An Advanced Signal Integrity Module tests impedance profile, intra-pair and inter-pair skew and crosstalk, while providing high-resolution insertion loss and eye diagrams.


Teledyne LeCroy

The RapidWave4000 has a breadth of test capabilities that fully satisfies high-volume, high-speed production test requirements, as well as the failure analysis tests needed for quality assurance. Its low-cost replaceable adapters enable the modules to connect to different cable types, while ensuring test consistency over many test cycles. A pay-per-test option can reduce capital equipment costs up to 40%. ■

Handheld Spectrum and Vector Network Analyzer Heads to the Field

SIGLENT TECHNOLOGIES RECENTLY introduced the SHA850A series, its first handheld spectrum and vector network analyzer. Highly integrated and specifically designed for field operation, the lightweight and portable device performs accurate measurements and offers flexible analysis capabilities. Able to handle advanced characterization or signal capture applications in harsh working environments, it provides professional accuracy with flexible analysis capabilities.

In spectrum-analyzer mode, it can measure up to 7.5 GHz. The DANL is as low as –165 dBm, which can effectively identify small signal levels. The single-sideband phase noise is ≤104 dBc/Hz @ 1 GHz with a 10-kHz offset; an independent full-frequency source and a 25-dB preamplifier is standard.

The SHA850A series' measurable frequency range in vector-network-analyzer mode and cable- and antenna-measurement mode spans 100 kHz to 7.5 GHz, with a dynamic range as high as 114 dB. This critical range suits the SHA850A series for applications such as measuring the passband and out-of-band rejection performance of filters at the same time, as well as measuring narrowband devices with high rejection. ■

Modular Solutions for Flexible Reliability Testing

Industry Applications

Compound Semiconductor R&D
Commercial Wireless
Military & Aerospace
Alternative Energy
Automotive
Telecom
Satcom
Space

Test Solutions

Device Characterization
RF & DC Accelerated Life Testing
Microwave/mm-Wave Test Fixtures
High Voltage Switching Life Testing
HTOL/HTRB/Burn-in Testing

Accel-RF
Instruments Corporation

4380 Viewridge Ave., Ste D
San Diego, CA 92123
858-278-2074
info@accelrf.com
www.accelrf.com

Software-Defined Front End Empowers Next-Gen Wireless Solutions

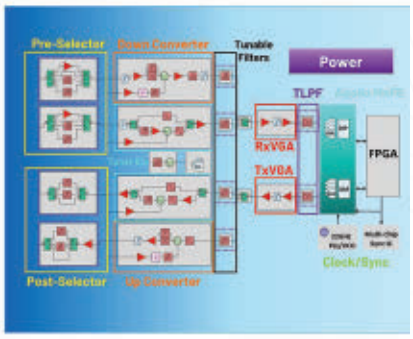

Features of the Apollo MxFE 4T4R include on-chip DSP, real-time FFT sniffer, full-rate programmable FIR filter, 128-tap complex FIR filter, fast-hopping NCOs, DDCs/DUCs, and fractional sample-rate converter. Analog Devices

AS WIRELESS SOLUTIONS become ubiquitous, the need for advanced RF infrastructures and systems becomes more pressing. The growth of advanced portable devices to address the needs of business, industry, and society in data-intensive applications is pushing demand for wider bandwidths and more rapid processing and analysis of data in wireless systems, especially at the network edge. Designers today need to accelerate design cycles and bring products to market faster and more cost-effectively, while future-proofing their product designs.

To address this demand, Analog Devices launched the Apollo MxFE, an advanced software-defined, direct RF-sampling, wideband mixed-signal front-end platform. The solution enables higher-speed data conversion and processing capabilities, while reducing electronic testing complexity. Apollo MxFE helps empower next-generation applications like phased-array radar, signals intelligence, industrial IoT, advanced test and measurement, aerospace & defense, and remote instrumentation.

Embracing issues like application versatility and rapid customization, the Apollo MxFE provides instantaneous bandwidths up to 10 GHz while directly sampling and synthesizing frequencies up to 18 GHz. The 16-nm CMOS device leverages high-dynamic-range RF analog-to-digital converter (ADC) and RF digital-to-analog converter (DAC) cores, and the company claims it has the best spurious-free dynamic range and noise spectral density available.

According to Bryan Goldstein, Vice President, Aerospace and Defense, at ADI, "The flexibility and simplicity designed into the Apollo MxFE platform has the potential to transform future engineering design for intelligent edge devices. Demand for higher data rates with shorter latencies at lower overall system power is accelerating across industries. Apollo MxFE gives design engineers the flexibility to design for those requirements today, as well as an ability to enhance performance over time using simple, software-defined design changes."

Apollo MxFE Product Details

Presented as the industry's first integrated radio capable of directly serving the emerging 6G frequency bands from 7 to 15 GHz, the Apollo MxFE 4T4R product has four 12-bit RF ADCs with a sample rate up to 20 Gsamples/s, four 16-bit RF DACs with a sample rate up to 28 Gsamples/s, an RF input bandwidth from dc to 18 GHz (Ku-band), and an instantaneous bandwidth up to 10 GHz. Features include on-chip DSP, a real-time FFT sniffer, a full-rate programmable FIR filter, a 128-tap complex FIR filter, fast-hopping NCOs, digital up/downconverters (DUCs/DDCs), and a fractional sample-rate converter *(see figure)*.

The DSP is dynamically configurable to enable rapid changes between narrowband and wideband profiles without taking down the JESD link. The Apollo MxFE 8T8R offers eight RF ADCs with a sample rate up to 8 Gsamples/s, eight RF DACs with a sample rate up to 16 Gsamples/s, an RF input bandwidth up to 16 GHz, and an instantaneous bandwidth up to 3 GHz. The on-chip DSP offers similar features and functionality to the 4T4R device with double the number of digital blocks, which are all dynamically configurable.

Forming the core of a larger ecosystem of recently released ADI hardware and software products, Apollo MxFE is augmented by high-performance variable-gain amplifiers, ultra-low-noise LDO and Silent Switcher regulators, clocking, and multichip synchronization. Its ecosystem includes subsystems like a PLL/VCO synthesizer with a fundamental frequency output of up to 22 GHz, offering noteworthy noise performance, temperature stability (0.06 ps/°C), and less than 1-ps alignment resolution.

The Apollo MxFE integrates the LTM4702 8A µModule regulator with Silent Switcher 3 technology to achieve high efficiency and excellent wideband noise performance. It also has a 10-channel precision synchronizer for time alignment of SYSREF signals to within 5 ps, for simultaneous sampling across multiple Apollo MxFE units on the same card or across different chassis.

On top of that, the Apollo MxFE can support two-dimensional system synchronization (fanout and/or daisy-chain architectures) for very large systems. Companion TxVGA and RxVGA solutions provide +15 dB of gain and the transition from single-ended to differential on Rx as well as differential to single-ended on Tx, to simplify the connection to the RF front end.

Bringing Wi-Fi 6 to Cars

Fig. 1.

Fig. 2.

Wi-Fi 6E PROVIDES significantly more bandwidth because of the addition of the 6-MHz band *(Fig. 1)*, offering a major upgrade over the 2.4- and 5-GHz bands used by prior standards. The extra bandwidth can be very useful in the automotive space as cars become more connected. Wireless connectivity for IoT and consumer telematics are becoming standard car components rather than options.

The JODY-W4 from u-blox is designed to make the automotive developer's job easier *(Fig. 2)*. The module is built around Infineon's 89570/89570B chipset. The compact, 13.8- × 19.8-× 2.5-mm system has three antenna ports. It's also pin-compatible with the company's JODY family.

Moreover, the JODY-W4 supports Bluetooth. This includes Bluetooth LE as well as the Bluetooth LE 5.3 version with long-range capability. The module has Wi-Fi DFS master support with zero-wait, too. This allows the module to operate in areas where some Wi-Fi channels can't be used, such as airports.

The obvious applications of the module include Wi-Fi hotspot and Bluetooth audio support as well as telematics, including inside telematics control units (TCUs). The latter can provide a central data-collection and distribution environment. Bluetooth LE can be used to support keyless access to services. In addition, the system is able to deliver firmware-over-the-air-updates (FOTAs) for engine control units (ECUs).

Broadcom Launches Wi-Fi RF FEM with Integrated Wi-Fi 7 Access-Point Filtering

The Overview

Broadcom's FBAR integrated front-end module (FiFEM) for Wi-Fi access-point (AP) applications span Wi-Fi routers, residential gateways, and enterprise access points (APs). The FiFEM devices incorporate second-generation FBAR filter technology to provide superior 5- and 6-GHz band coexistence and low in-band insertion loss while significantly reducing the bill of materials (BOM) at the RF front end.

Who Needs It & Why?

To date, more than 60 countries have opened the 6-GHz band for Wi-Fi use, providing spectrum for connected Wi-Fi 6E and Wi-Fi 7 devices to maximize their capabilities. With the growing adoption of 6-GHz Wi-Fi in the market, the coexistence of 5- and 6-GHz signals is a critical consideration for Wi-Fi 6E and Wi-Fi 7 AP designs. Thus, designers of Wi-Fi APs will find broad applicability for Broadcom's FiFEM products.

Under the Hood

The FiFEM's integration of Broadcom's second-generation Wi-Fi FBAR filter delivers high 5/6-GHz band isolation and efficiency and avoids potential yield loss due to mismatched external filters. Further, power dissipation in 5- and 6-GHz RF chains can be substantial, especially in a conventional tri-band 4x4 Wi-Fi AP system where RF power can reach 10 W/band. The FiFEM device is the first nonlinear FEM qualified for Broadcom's Wireless FEM Active Management (WiFAM) Gen2 technology using advanced digital predistortion (DPD) technology with dynamic bias handling. Between the RF filter integration and DPD features, the FiFEM devices are highly optimized for Wi-Fi 7 APs.

In addition, the devices maintain a high-performance, nonlinear power amplifier (PA) design optimized for Broadcom's Wi-Fi SoC DPD operation, enabling up to 40% reduction in RF front-end power. This enhances gateway energy efficiency in terms of average power consumption.

The FiFEM family comprises four products in conventional FEM packages (3×5 mm^2):

- AFEM-W750-MP1 (5 GHz, +23 dBm)
- AFEM-W750-HP1 (5 GHz, +25 dBm)
- AFEM-W760-MP1 (6 GHz, +23 dBm)
- AFEM-W760-HP1 (6 GHz, +25 dBm)

Broadcom has begun shipping samples of the AFEM-W750 and AFEM-W760 to early access customers and partners.

Phase-Noise Modeling, Simulation, and Propagation in Phase-Locked Loops (Part 1)

This three-part series discusses how phase noise in general is modeled and simulated, and how RF component phase noise propagates through a PLL to determine its output phase noise.

By Frederick Weist,
Principal, FCW Sciences

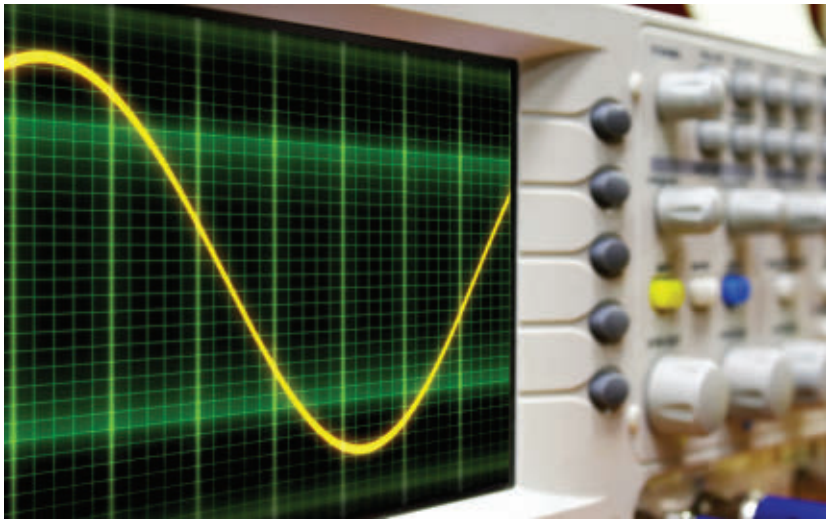

Dreamstime_Alexey-Filatov_75968986

Phase-locked loops (PLLs) are ubiquitous in today's high-tech world. Almost all commercial and military products employ them in their operation, and phase (or PM) noise is a major concern. Frequency (or FM) noise is closely related (instantaneous frequency is the time derivative of phase) and generally considered under the umbrella of phase noise (perhaps both might be considered "angle noise"). Amplitude (or AM) noise is another consideration.

While both affect PLL performance, amplitude noise is usually self-limiting and of no consequence. Phase noise, therefore, at the PLL output and of the RF components, is the dominant concern. Of course, output phase noise is the ultimate concern—it depends critically on the phase noise of each component.

A number of factors contribute to component phase noise, such as power supplies, EMI, and semiconductor anomalies, to name a few. Understanding these factors allows us to implement mitigation strategies for component phase noise and, ultimately, output phase noise.

The kind of PLL we're discussing is of the analog hardware variety rather than the digital or software variety. The general topology of such a PLL is a single-loop system that contains a precision reference, reference divider, feedback divider, possible prescaler, voltage or current (aka charge pump) phase detector, loop filter, and voltage-controlled oscillator (VCO). These components may all be discrete or some of them may be contained in an IC. In any event, we show how phase noise in general can be analyzed and how RF component phase noise propagates through a PLL to determine its output phase noise.

In Part 1, we discuss some brief theory and typical measurements of phase noise along with the analysis (modeling, simulation, and propagation) thereof, and show in detail the method used by most computer-aided-design (CAD) applications.

Brief Theory and Typical Measurements of Phase Noise

Phase noise is an important and complex subject with ongoing research as well as a tenuous understanding of its origins and a questionable mathematical foundation. However, a number of approximations and workarounds are utilized to produce excellent theoretical and practical results.[1,2,3] It's a mature subject with much literature available. Several instruments are available that accurately measure phase noise, and innumerable fielded systems with PLLs have controlled phase-noise characteristics.

Here, we briefly review the theory of phase noise in the time and frequency domains as well as the transformation between

domains for both the baseband (BB) realm (BB noise signal that phase-modulates the RF carrier signal) and the RF realm (RF carrier signal that's phase-modulated by the BB noise signal).

Also, we summarily review the typical measurements of phase noise for both realms in the frequency domain, which are, of course, different equivalent representations of the same phenomenon and give the same result.

The BB realm is considered the less important realm, but is of interest for the origins of phase noise and offers better measurement accuracy than the RF realm. The RF realm is considered the more important realm and is of interest for the observable manifestations of phase noise, though it has inferior measurement accuracy to the BB realm.[1,8] In addition, we investigate the equivalency of both types of measurements.

As is well known in all of physics, there are deterministic and non-deterministic (aka random, stochastic or probabilistic) processes. In PLLs, these processes are signals, which can be expressed in both the time and frequency domains for both realms, with the two domains related through transform theory by the Fourier transform.

To use (in this case, continuous) transform theory, a system is modeled as a (continuous) linear time-invariant network, which means a PLL must be in a locked state. In contrast, the model of a PLL in an unlocked state is nonlinear; thus, transform theory cannot be applied.

Moreover, the transformation between domains is direct for deterministic signals and indirect for random signals. Direct means the transformation is done directly between the time and frequency domains because the direct transform exists. Indirect means that there's an intermediate step in the transformation between domains, which is to calculate the autocorrelation function of the random signal and take its time-average, and then take the transform, because the direct transform doesn't exist.[6]

Phase noise, then, in an RF system or an RF component, is produced when an internal and/or external BB random (noise) signal, of both known and unknown origin, phase-modulates a system's or a component's internal RF deterministic (carrier) signal. It follows, of course, that phase noise, being a random phenomenon or signal, is imbued with an indirect transformation.

Generally, for a random signal in the frequency domain, the spectrum as a voltage spectral density (VSD) doesn't exist. However, the spectrum does exist as a power spectral density (PSD) having only magnitude and no phase information. In contrast, for a deterministic signal in the frequency domain, the spectrum generally does exist as a VSD, having both magnitude and phase information, which also, of course, has a PSD by extension.

Moreover, in the frequency domain for the BB realm, the spectrum is a low-pass (or quasi-low-pass) function, and for the RF realm the spectrum is a bandpass function. Additionally, in this discussion, we're working with only positive one-sided (OS) spectra and positive single-sideband (SSB) phase-noise information in contrast to two-sided (TS) spectra and double-sideband (DSB) phase-noise information.

We also note that in the time domain, phase noise is typically referred to as phase jitter and in the frequency domain it's typically referred to as stated-phase noise. The phenomenon in both domains is related through the definition of instantaneous frequency being the time derivative of phase.[1,8,10]

With the above background in mind, we briefly review some theory in the time and frequency domains as well as the transformation between domains *for the BB realm*. In this realm, our theory and analysis basically exist in principle since there's no analytical expression for our random (noise) signal in the time domain (which is where our analysis begins). Hence, after transformation, there's no analytical expression in the frequency domain. We have the following mathematical representations and transform steps:[6,7,8]

1. The *time domain function or phase waveform*, which is a real (non-complex) random process with a zero-mean Gaussian probability density function, $\phi(t)$:

$$\phi(t) = \text{random process (rad)} \qquad (1)$$

where t is the time.

2. The autocorrelation function of (1), $R_\phi(t, \tau)$:

$$R_\phi(t,\tau) = \mathrm{E_{op}}\{\phi(t)\phi(t+\tau)\} \ (\mathrm{rad^2}) \qquad (2)$$

where τ is the positive time increment between measurements and $\mathrm{E_{op}}\{...\}$is the statistical average operator.

3. The Fourier transform of the time-average of Equation 2, giving the unnormalized (UN) BB *frequency domain function* or PSD, $W_\phi(\xi)$ or $WdB\phi(\xi)$:

$$W_\phi(\xi) = \mathrm{F_{op}}\left\{\mathrm{A_{op}}\{R_\phi(t,\tau)\}\right\} \ \left(\frac{\mathrm{rad^2}}{\mathrm{Hz}}\right) \ \Rightarrow$$

$$WdB_\phi(\xi) = 10 \ \mathrm{Log}\, W_\phi(\xi) \ \left(\frac{\mathrm{dBm}}{\mathrm{Hz}}\right) \qquad (3)$$

where ξ is the frequency, $\mathrm{A_{op}}\{...\}$is the time average operator, and $\mathrm{F_{op}}\{...\}$ is the Fourier transform operator. Typical plots of the phase waveform and its UN BB PSD are shown in *Figure 1a and 1b*.

Next, we briefly review similar theory in the time and frequency domains as well as the transformation between domains *for the RF realm*. In this realm, our theory and analysis are fairly analytical since there's a fairly analytical expression for our deterministic (carrier) signal in the time domain (which, once again, is where our analysis begins). Hence, after transformation, there's a fairly analytical expression in the frequency domain.

For a "reasonable" phase waveform deviation (aka small angle..., small modulation index..., or narrowband PM...approximation) of ≤ 0.2 rad (≤ 11.5°), where a PM spectrum is basically identical to a DSB AM spectrum—which is the case for

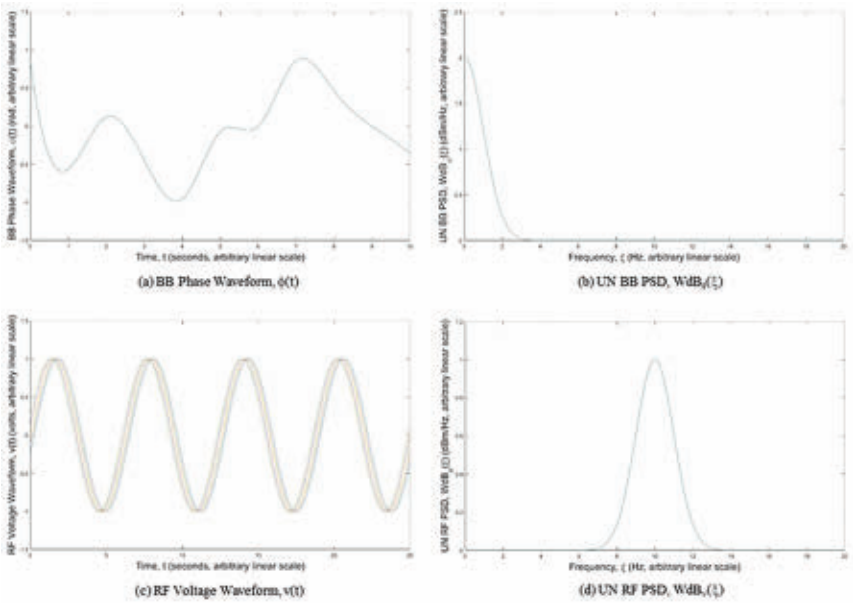

1. Typical plots in phase-noise theory of (a) the baseband (BB) phase waveform, $\phi(t)$, (b) the unnormalized (UN) BB power spectral density (PSD), $Wdb_\phi(\xi)$, (c) the RF voltage waveform, $v(t)$, and (d) the UN RF PSD, $Wdb_v(\xi)$.

all practical phase noise issues—we have the following mathematical representations and transform steps (details not shown for brevity):[7,8,10]

4. The *time domain function or voltage waveform* (also a function of the BB parameters), $v(t)$:

$$v(t) = V\cos[2\pi f_0 t + \Theta + \phi(t)] \text{ (volts)} \qquad (4)$$

where V is the statistical mean amplitude, f_0 is the carrier frequency, and Θ is the initial phase (V is a special case of the general amplitude, $V + a(t)$, where $a(t)$ is the statistical zero-mean amplitude noise with $a(t) = 0$, since, as mentioned, it's self-limiting and of no consequence):

5. The autocorrelation function of Equation 4 (again also a function of the BB parameters), $R_v(\tau)$:

$$R_v(\tau) = \frac{V^2 e^{-\Omega^2}}{2}\cos(2\pi f_0\tau) \text{ with } \Omega^2 \equiv R_\phi(0) - R_\phi(\tau) \text{ (volts}^2\text{)} \qquad (5)$$

where $R_\phi(0)$ is $R_\phi(\tau)$ with $\tau = 0$, which is the variance of $\phi(t)$.

6. The Fourier transform of the time average of Equation 4 (once again also a function of the BB parameters) giving the UN RF *frequency domain function* or PSD, $W_v(\xi)$ or $WdB_v(\xi)$:

$$W_v(\xi) = \frac{V^2 e^{-\sigma^2}}{2}\left[\delta(\xi - f_0) + W_\phi(\xi - f_0)\right] \text{ with } \sigma^2 \equiv R_\phi(0) = \int_0^\infty W_\phi(\xi)\,d\xi \left(\frac{\text{volts}^2}{\text{Hz}}\right) \Rightarrow$$

$$WdB_v(\xi) = 10\,\text{Log}\,W_v(\xi)\left(\frac{\text{dBm}}{\text{Hz}}\right) \qquad (6)$$

where $d(\xi - f_0)$ is the Dirac delta or unit impulse function and $W_\phi(\xi - f_0)$ is the UN BB PSD, $W_\phi(\xi)$, translated from the BB realm to the RF realm through the modulation process. Typical plots of the voltage waveform and its UN RF PSD are shown in *Figure 1c and 1d*.

It should be noted that if $\phi(t)$ is strict-sense stationary (a reasonable assumption), it may be proved that $v(t)$ is at least wide-sense stationary. In this case, the Weiner-Khinchin theorem holds, with $R_\phi(t, \tau)$ and $R_v(t, \tau)$ becoming functions only of τ, [$R_\phi(t, \tau) \rightarrow R_\phi(\tau)$ and $R_v(t, \tau) \rightarrow R_v(\tau)$] and therefore finding the time-averages of $R_\phi(\tau)$ and $R_v(\tau)$ aren't necessary. Hence, $W_\phi(\xi)$ and $W_v(\xi)$ are the Fourier transforms of $R_\phi(\tau)$ and $R_v(\tau)$ themselves.[1,6,7,9]

Then, with the above brief theory in mind, we summarily review the typical measurements of phase noise for both the BB and RF realms in the frequency domain.

Measurement in the BB Realm

In the UN BB PSD above, a particular frequency is selected and its power in a 1-Hz bandwidth is divided by the total integrated power over the low-pass spectrum, which gives the normalized (NM) BB PSD, $L_\phi(\xi)$ or $LdB_\phi(\xi)$:

$$L_\phi(\xi) \equiv \frac{W_\phi(\xi)}{2P_z}\left(\frac{\text{rad\_ratio}^2}{\text{Hz}}\right) \Rightarrow LdB_\phi(\xi) = 10\,\text{Log}\,L_\phi(\xi)\left(\frac{\text{dBz}}{\text{Hz}}\right) \qquad (7)$$

where ξ is the particular frequency, P_z is the total integrated low-pass power, and dBz is decibels relative to P_z. *The measurement is indirect, using a signal source analyzer*, which demodulates, measures, processes, and displays the BB signal to produce $L_\phi(\xi)$ or $LdB_\phi(\xi)$ [$W_\phi(\xi)$ contains DSB information and therefore the factor of 2 is needed in the calculation of $L_\phi(\xi)$ to give SSB information]. It's considered more accurate than that done in the RF realm.[1,8]

Measurement in the RF Realm

In the UN RF PSD above, a particular offset frequency from the carrier is selected. Its power in a 1-Hz bandwidth is divided by the total integrated power over the bandpass spectrum, which gives the NM RF PSD, $L_v(f)$ or $LdB_v(f)$:

$$L_v(f) \equiv \frac{W_v(f + f_0)}{P_c}\left(\frac{\text{volts\_ratio}^2}{\text{Hz}}\right) \Rightarrow LdB_v(f) = 10\,\text{Log}\,L_v(f)\left(\frac{\text{dBc}}{\text{Hz}}\right) \qquad (8)$$

where f is the particular offset frequency from the carrier ($f = \xi - f_0$ with $\xi \geq f_0$), P_c is the total integrated bandpass power, and dBc is decibels relative to P_c. *The measurement is direct, using a spectrum analyzer* with phase-noise processing capability, which measures, processes, and displays the RF signal to produce $L_v(f)$ or $LdB_v(f)$. It's considered less accurate than that done in the BB realm.[1,8]

Fast Pulse Test Systems from Avtech

Avtech offers over 500 standard models of high-speed pulsers, drivers, and amplifiers ideal for both R&D and automated factory-floor testing. Some of our standard models include:

AVR-E3-B: 500 ps rise time, 100 Volt pulser

AVRQ-5-B: Optocoupler CMTI tests, >120 kV/us

AVOZ-D6-B: 1000V / 200A, 1-10 us pulser

AV-1010-B: General purpose 100V, 1 MHz pulser

AVO-9A-B: 200 ps t_r, 200 mA laser diode driver

AV-156F-B: 10 Amp current pulser for airbag initiator tests

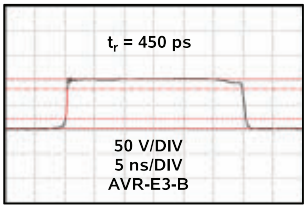

AVTECH

Nanosecond Electronics
Since 1975

Pricing, manuals, datasheets and test results at:
www.avtechpulse.com

AVTECH ELECTROSYSTEMS LTD.
US & Canada 888-670-8729, Worldwide +1-613-686-6675
info@avtechpulse.com

High Output - Low Risetime Pulsers from Avtech

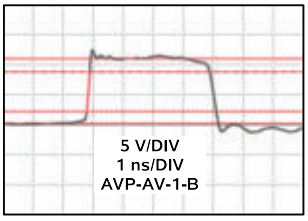

Nanosecond and faster pulsers covering a wide range of amplitudes!

GPIB / RS-232 / Ethernet standard on "-B" models.

Standard and customized models available.

Ampl	t_{RISE}	Max. PRF	Model
5 V	80 ps	1 MHz	AVP-AV-1S-C
10 V	120 ps	1 MHz	AVP-AV-1-B
20 V	120 ps	1 MHz	AVP-AV-HV2-B
20 V	200 ps	10 MHz	AVMR-2D-B
40 V	150 ps	1 MHz	AVP-AV-HV3-B
50 V	500 ps	1 MHz	AVR-E5-B
100 V	500 ps	100 kHz	AVR-E3-B
100 V	300 ps	20 kHz	AVI-V-HV2A-B
200 V	1 ns	50 kHz	AVIR-1-B
200 V	2 ns	20 kHz	AVIR-4D-B
400 V	2.5 ns	2 kHz	AVL-5-B-TR

AVTECH

Nanosecond Electronics
Since 1975

Pricing, manuals, datasheets and test results at:
www.avtechpulse.com

AVTECH ELECTROSYSTEMS LTD.
US & Canada 888-670-8729, Worldwide +1-613-686-6675
info@avtechpulse.com

Pulsed Laser Diode Drivers from Avtech

Each of the 18 models in the Avtech **AVO-9 Series** of pulsed laser diode drivers includes a replaceable output module with an ultra-high-speed socket, suitable for use with sub-nanosecond pulses.

Models with maximum pulse currents of 0.2A to >10A are available, with pulse widths from 400 ps to 1 us.

GPIB, RS-232, and Ethernet control available.

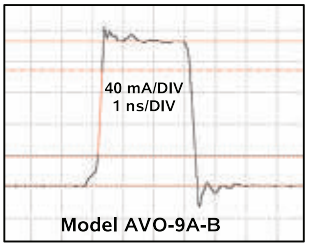

AVTECH

Nanosecond Electronics
Since 1975

Pricing, manuals, datasheets and test results at:
www.avtechpulse.com/laser

AVTECH ELECTROSYSTEMS LTD.
US & Canada 888-670-8729, Worldwide +1-613-686-6675
info@avtechpulse.com

100 to 1000 Volt Lab Pulsers

Avtech offers a full line of 100, 200, 500, 700 and 1000 Volt user-friendly pulsers capable of driving impedances of 50 Ω and higher. The **AVR Series** is suitable for semiconductor and laser diode characterization, time-of-flight applications, attenuator testing, and other applications requiring 10, 20, or 50 ns rise times, pulse widths from 100 ns to 100 us, and PRFs up to 100 kHz. GPIB, RS-232, and Ethernet ports are standard.

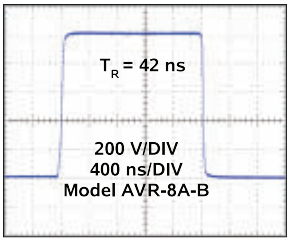

See additional test results at:
http://www.avtechpulse.com/medium

AVTECH

Nanosecond Electronics
Since 1975

Pricing, manuals, datasheets and test results at:
www.avtechpulse.com/medium

AVTECH ELECTROSYSTEMS LTD.
US & Canada 888-670-8729, Worldwide +1-613-686-6675
info@avtechpulse.com

Equivalency of Both Measurements

As mentioned, $L_\phi(\xi)$ or $LdB_\phi(\xi)$ and $L_v(f)$ or $LdB_v(f)$ are different representations of the same phenomenon and logically should give the same result for all practical phase-noise issues (where, also as mentioned, the phase deviation is considered "reasonable"). Therefore, for this case, they're equivalent and do give the same result, which is termed the NM PSD, $L(f)$ or $LdB(f)$. The BB and RF realm subscripts (ϕ and v) are dropped and no subscripts are used (even the "reasonable" condition has some anomalies where approximations with academic and practical arguments must be used):[1,10]

$$L_\phi(\xi) = L_v(f) \equiv L(f) \ \left(\frac{\text{volts\_ratio}^2}{\text{Hz}}\right) \ \Rightarrow$$
$$LdB_\phi(\xi) = LdB_v(f) \equiv LdB(f) \ \left(\frac{\text{dBc}}{\text{Hz}}\right) \quad (9)$$

where the typical display has f as the offset frequency from the carrier for the x-axis in units of Hz on a logarithmic scale and $LdB(f)$ as the NM RF PSD for the y-axis in units of dBc/Hz on a linear scale, for both the indirect and direct measurements mentioned above, to ultimately relate everything to the RF realm *(Fig. 2)*.

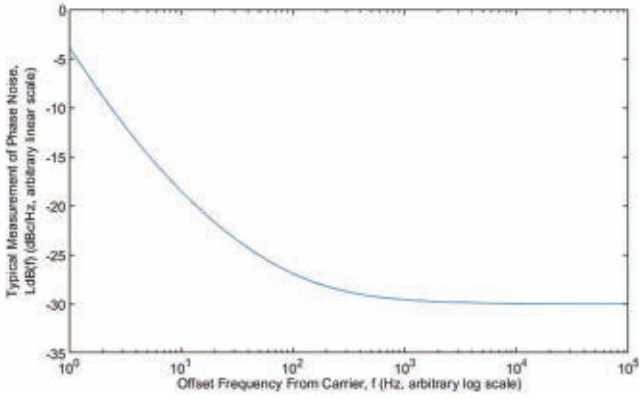

2. Typical measurement of phase noise for both the baseband and RF realms in the frequency domain.

It should be noted that if the "reasonable" condition isn't met, then Bessel function mathematics must be used to relate $L_\phi(\xi)$ to $L_v(f)$. Therefore, both measurements would not be equivalent, would give different results, and would be considered a catastrophic problem.

Analysis (Modeling, Simulation, and Propagation) of Phase Noise=

Armed with the above information, we now come to the analysis of phase noise in a PLL and how it's modeled and simulated in general. Also discussed is how RF component phase noise is propagated through the PLL to determine its output phase noise. Typically, phase noise is effectively modeled using the "General Phase Noise Model" *(Fig. 3)* with its standard integer power series:

$$L(f) = \sum_{j=0}^{4} L_j(f) \ \text{ with } \ L_j(f) = \frac{h_j}{f^j} \ \left(\frac{\text{volts\_ratio}^2}{\text{Hz}}\right) \ \Rightarrow \ LdB(f) = 10 \ \text{Log} \ L(f) \ \left(\frac{\text{dBc}}{\text{Hz}}\right) \quad (10)$$

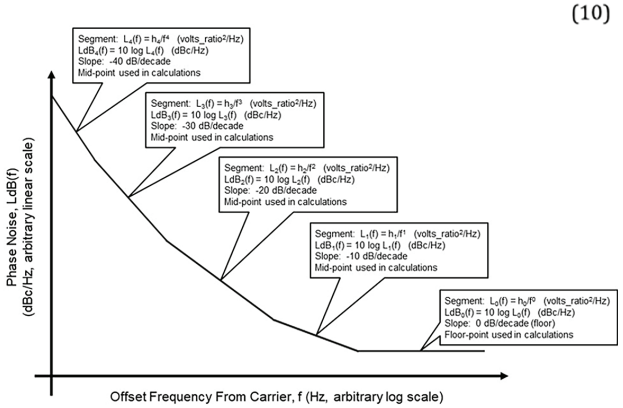

3. General Phase Noise Model used in the analysis (modeling, simulation, and propagation) of phase noise.

where h is a weighting coefficient and f is the offset frequency from the carrier.[1,7] It's then simulated with any standard application (in this case, we use MATLAB). Finally, propagation of component phase noise through the PLL to determine its output phase noise is done using the *General PLL Block* "Diagram & Phase Noise Propagation Model" *(Fig. 4)*.

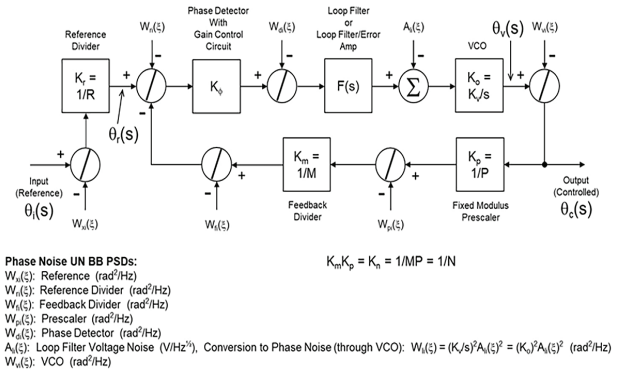

4. General PLL block diagram and Phase Noise Propagation Model used in the analysis (modeling, simulation, and propagation) of phase noise.

Furthermore, to simplify the analysis, all components' phase noise is approximated as being uncorrelated (a reasonable assumption) so that their NM PSDs add directly, rather than having to deal with correlated signals, which significantly complicates the analysis. Analysis is then done with the following *Phase Noise Analysis Procedure*:[4,5]

1. The PLL must be represented as a (in this case continuous) linear, time-invariant network, which means it must be locked at one of its outputs.

2. All components' phase noise must be approximated as being uncorrelated.

Solutions That Are Above and Beyond

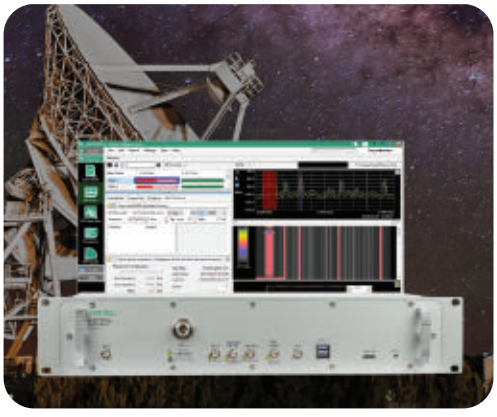

Remote Spectrum Monitor
MS27201A

Interference Monitoring to 54 GHz

Our family of remote spectrum monitors with Vision PC software allow for automated inference detection over wide geographical areas. Protect your spectrum from illegal transmitters and interferers with 24/7 monitoring and long-term trace logging. Monitor multiple nodes, collect spectrum history, identify signal patterns, and conduct coverage mapping using the advanced Vision PC software.

Locate and Analyze

Field Master Pro™
MS2090A

We've Got You Covered

Our Field Master Pro handheld spectrum analyzers are built to deliver in the toughest environments and offer leading edge performance up to 54 GHz and 110 MHz analysis bandwith. With a large 10 inch touch screen for quick and easy setup and results display, ruggedized case, and battery operation, you can be confident of getting the job done wherever you go.

IQ Capture and Streaming up to 110 MHz Bandwidth

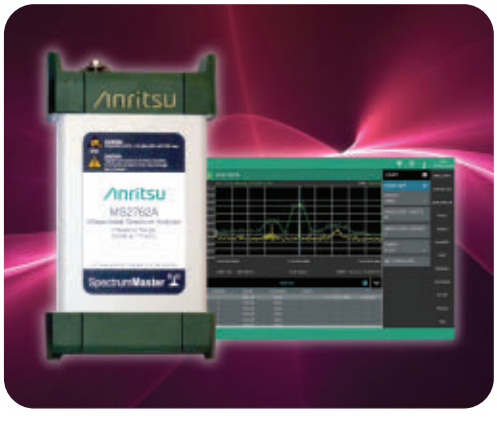

Spectrum Master™
MS2760A

Ultra-Portable Ultra-Broadband Up to 170 GHz

Anritsu's Spectrum Master MS276xA is a family of direct connect broadband spectrum analyzer solutions that deliver superior dynamic range and higher sensitivity in the millimeter-wave bands in a form factor that fits in your pocket! Nothing on the market comes close.

mmWave Test and Measurement for Radio Astronomy, Automotive Radar, Satellite Radio Links, WIGig, and More

Anritsu
Advancing beyond

Discover how you can achieve measurement confidence with Anritsu.
Visit **www.anritsu.com/test-measurement**

3. Each component's phase-noise plot is obtained from its datasheet and the "General Phase Noise Model" *(Fig. 3)* is fit to each component's plot to determine the segments of the general model (some of which may not exist) that match each component's plot.

4. For each component's fitted General Phase Noise Model, one phase noise point, $LdB_j(f_k)$ $(j,k = 0,a;\ 1,b;\ 2,c;\ 3,d;\ 4,e)$, within each segment is obtained for use in calculations (the mid-point within a segment is often used). Convert all log values to linear values, $LdB_j(f_k)$ Þ$L_j(f_k)$:

$$LdB_j(f_k) = 10\ \mathrm{Log}\ L_j(f_k)\ \left(\frac{\mathrm{dBc}}{\mathrm{Hz}}\right) \Rightarrow L_j(f_k) = 10^{\frac{LdB_j(f_k)}{10}} = \frac{h_j}{f_k^j}$$

$$(j,k = 0,a;\ 1,b;\ 2,c;\ 3,d;\ 4,e)\ \left(\frac{\mathrm{volts\_ratio}^2}{\mathrm{Hz}}\right) \qquad (11)$$

5. Each component's fitted General Phase Noise Model coefficients, h_j, are calculated using the phase-noise points from step 4 (some of which may be zero):

$$h_j = L_j(f_k) f_k^j\ \ (j,k = 0,a;\ 1,b;\ 2,c;\ 3,d;\ 4,e)\ \left(\mathrm{volts\_ratio}^2 \mathrm{Hz}^{j-1}\right) \qquad (12)$$

6. Each component's fitted General Phase Noise Model coefficients, h_j, from step 5 are used to form each component's phase-noise model, $L_{ci}(f)$:

$$L_{ci}(f) = \sum_{j=0}^{4} L_j(f) \text{ with } L_j(f) = \frac{h_j}{f^j}\ \left(\frac{\mathrm{volts\_ratio}^2}{\mathrm{Hz}}\right) \qquad (13)$$

which can be simulated to produce component phase noise curves.

7. Each component's phase-noise model, $L_{ci}(f)$, from step 6 is multiplied by its applicable transfer function (output or error; to be discussed later) magnitude-squared, $|T(f)|^2$, to get its propagated phase noise model, $L_{co}(f)$:

$$L_{co}(f) = L_{ci}(f)|T(f)|^2\ \left(\frac{\mathrm{volts\_ratio}^2}{\mathrm{Hz}}\right) \qquad (14)$$

which can be simulated to produce component propagated phase-noise curves.

8. Each component's propagated phase noise model, $L_{co}(f)$, from step 7 is summed together with all others to get the output phase noise model, $L_{to}(f)$:

$$L_{to}(f) = \sum L_{co}(f)\ \left(\frac{\mathrm{volts\_ratio}^2}{\mathrm{Hz}}\right) \Rightarrow LdB_{to}(f) = 10\ \mathrm{Log}\ L_{to}(f)\ \left(\frac{\mathrm{dBc}}{\mathrm{Hz}}\right) \qquad (15)$$

which can be simulated to produce the output phase noise curve.

This, then, is our phase-noise analysis (modeling, simulation, and propagation) procedure. As mentioned, it's the method used by most CAD applications for phase-noise analysis.

The previous information will be used in the upcoming Part 2, where we design a hypothetical PLL frequency synthesizer as an example to be used for analysis. ■

ALSO CHECK OUT PART 2 AND PART 3.

REFERENCES

1. F.M. Gardner, "Phaselock Techniques", 3rd ed., John Wiley, Hoboken, NJ, 2005.
2. R.E. Best, "Phase-Locked Loops, Design, Simulation and Applications", 6th ed., McGraw-Hill, New York, NY, 2007.
3. P.V. Brennan, "Phase-Locked Loops: Principles and Practice", McGraw-Hill, New York, NY, 1996.
4. E. Drucker, "Phase Lock Loops and Frequency Synthesis for Wireless Engineers", 1997, Frequency Synthesis & Phase-Locked Loop Design, 3 Day Short Course, Besser Associates, Mountain View, Calif., 1999.
5. F.C. Weist, "Phase Locked Loop Basics for Frequency Synthesizer Applications", Short Course, Clarksburg, Md., 2011.
6. P.Z. Peebles, Jr., "Probability, Random Variables and Random Signal Principles"', McGraw-Hill, New York, NY, 1980.
7. A. Godone, S. Micalizio, and F. Levi, "RF spectrum of a carrier with a random phase modulation of arbitrary slope", Istituto Nazionale di Ricerca Metrologic, INRIM, Strada delle Cacce 91, 10135 Torino, Italy, Metrologia, vol. 45, pp. 313-324, BIPM and IOP Publishing Ltd., Bristol BS1 6HG, UK, May 2008.
8. B. Nelson, "Phase noise 101: basics, applications and measurements", Keysight Technologies, 2018.
9. A. El Gamal, EE278 Lecture Notes 7: "Stationary random processes", Dept. of Electrical Engineering, College of Engineering, Stanford University, Stanford, CA, Autumn 2015.
10. K. J. Button, ed., Infrared and Millimeter Waves, Volume 11: Millimeter Components and Techniques, Part III, Chapter 7: "Phase Noise and AM Noise Measurements in the Frequency Domain", A. L. Lance, W. D. Seal and F. Labaar, TRW Operations and Support Group, One Space Park, Redondo Beach, CA, Academic Press, Cambridge, MA, 1984.

OUT OF THIS WORLD PERFORMANCE

Introducing the
HLM-8010CSP1
MMIC DC to
40 GHz Limiter

Marki Microwave continues to push the frequency envelope with its chip scale packaging (CSP) portfolio, featuring game-changing, die-level performance in an ultra-compact 1.5 x 1.5 mm surface mount package.

- **CSP compatible with standard pick-and-place assembly**
- **+8 dBm flat leakage at 40 GHz**
- **0.5 dB typical insertion loss**
- **+11 dBm typical P1dB**
- **16 dB minimum return loss across band**

The Trusted Leader When Performance Matters

Contact: sales@markimicrowave.com

www.markimicrowave.com

Marki® microwave

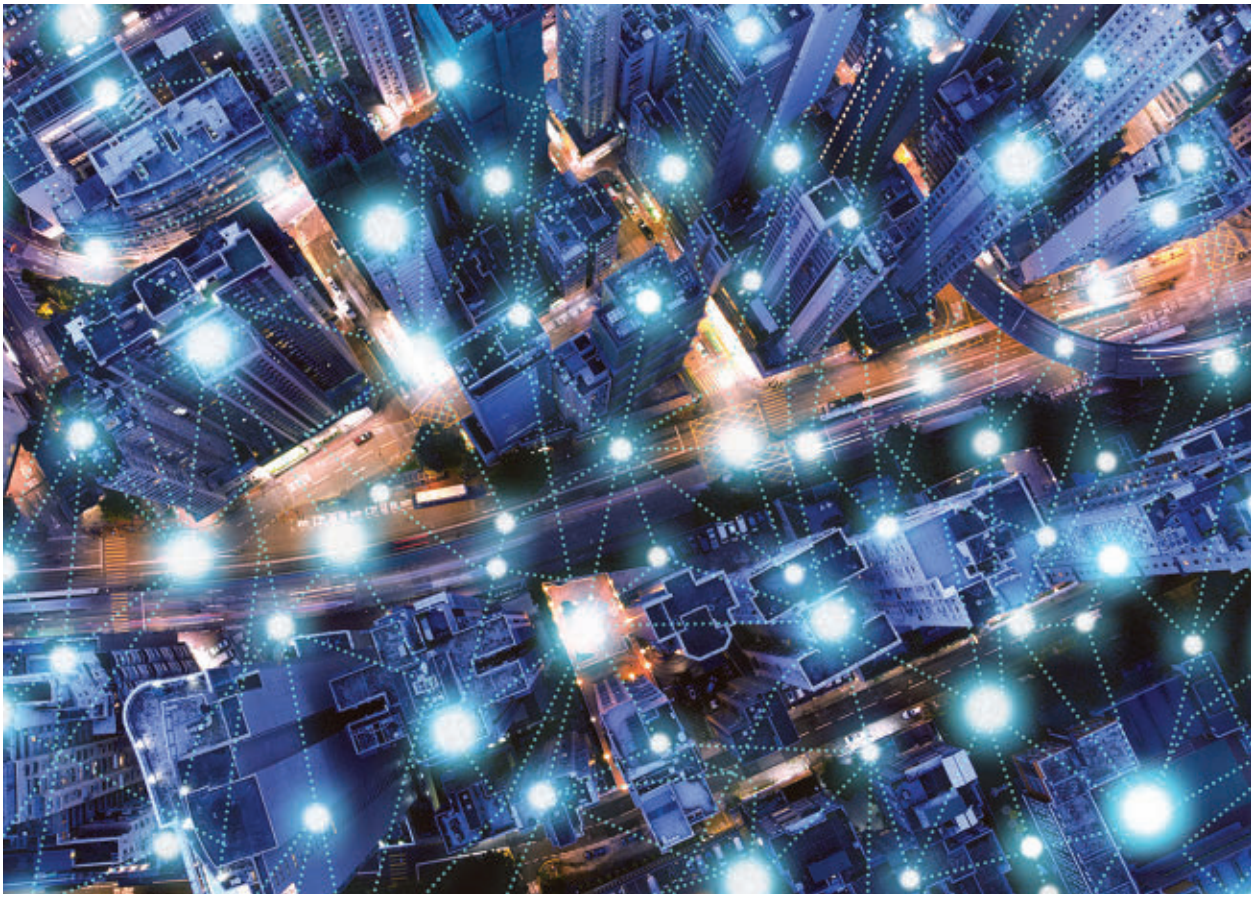

Dreamstime_Kiyoshi-Hijiki_180331688

What's the Difference Between Wi-Fi HaLow and Bluetooth?

As the IoT's reach into daily life is extended, it's important to understand the various wireless protocols that meet the unique needs of IoT environments.

By Michael De Nil, *Co-Founder & CEO, Morse Micro*

Today, the Internet of Things (IoT) is relevant to almost every industry and is one of the fastest-growing sectors of IT. Last year, spending on IoT reached a whopping $300.3 billion and it's expected to reach USD $650.5 billion by 2026.

With the world of IoT becoming an essential part of our lives, businesses must understand how to support the growing connectivity needs that come with this new era.

Not All Connections are the Same

The first thing to note is that not all connectivity is the identical. Wi-Fi HaLow, which incorporates IEEE 802.11ah and is one of the latest Wi-Fi protocols in the IEEE 802.11 family, was engineered specifically to meet the unique needs of IoT environments.[1]

Wi-Fi HaLow facilitates a more comprehensive approach to IoT wireless connectivity. It can deliver all of the benefits that consumers have come to expect from Wi-Fi today, while providing a tenfold increase in connectivity range as well as

The practical range of any wireless protocol also depends on physical barriers or obstacles between devices.

significantly lower power consumption for thousands of devices connected to the same access point. Like other modern Wi-Fi technologies, Wi-Fi HaLow also allows for multi-vendor interoperability, easy setup without disrupting existing Wi-Fi networks, and the latest Wi-Fi security.

What About Bluetooth?

Bluetooth is a popular wireless personal-area-network (WPAN) protocol used in many consumer devices such as smartphones, wireless headphones, and portable speakers for short-range communication. It is unlikely to support IoT use cases that rely on large numbers of low-power devices connected over long distances.

This comparison considers two separate Bluetooth versions: Bluetooth Classic and Bluetooth Low Energy (BLE), also known as Bluetooth 4.0. The *table (right)* presents a comparison of Wi-Fi HaLow with Bluetooth, showing how the two protocols stack up.

Going the Distance

Wi-Fi HaLow operates in the sub-1-GHz band with narrower channels (from 1 to 16 MHz), while Wi-Fi 4, 5, and 6 use channels with bandwidths from 20 to 160 MHz. The lower RF frequencies of Wi-Fi HaLow, which range from 850 to 950 MHz (compared to 2.4 or 5 GHz for Wi-Fi 4 or Wi-Fi 6), and range-optimized modulation and coding schemes, enable Wi-Fi HaLow devices to exceed a range of 1 km.[2]

By comparison, the Bluetooth standard operates in the 2.4-GHz ISM band and may support a maximum range of about 100 meters outdoors with no obstructions. However, most Bluetooth-enabled consumer devices operate indoors and at shorter ranges, generally 9 to 12 meters.

The latest Bluetooth version 5.0 offers a long-range mode known as Coded PHY. It enables Bluetooth connectivity to range beyond even 1 km outdoors with no obstructions but at a low fixed 125-kb/s data rate.

The practical range of any wireless protocol also depends on physical barriers or obstacles between devices. As a sub-1-GHz protocol, Wi-Fi HaLow offers exceptional penetration through obstacles of materials such as glass, wood, metal mesh, or concrete. By comparison, Bluetooth signals in the 2.4-GHz band experience more attenuation and are more easily blocked by obstacles than Wi-Fi HaLow signals.

Capacity Counts

A single Wi-Fi HaLow access point (AP) can handle thousands of connected devices. This capacity is a key feature when it comes to handling the huge number of IoT devices for larger-scale deployments in commercial buildings, factories, and other industrial applications. In a home setting, a single Wi-Fi HaLow AP can easily scale to meet the IoT demands of a typical household.

While the stated capacity for standard Bluetooth connectivity is up to seven devices, the practical capacity tends to be in the range of three or four devices. BLE offers greater capacity, but not by much. The practical limit for a central BLE device is about 20 devices. For this reason, BLE requires a mesh network to handle a larger number of devices.

Bluetooth Mesh was developed to meet that need, enabling the development of large-scale networks where hundreds or even thousands of Bluetooth devices can communicate with one another. However, because the payload of a Bluetooth mesh packet is small at 11 bytes, segmentation must be used to send larger packets, and packet size and number of mesh hops adversely affect packet latency.[3]

	Bluetooth	Wi-Fi HaLow
Reach	Classic: 50 m BLE and V4: up to 100 m BLE 5: up to 400 m	1 km
Capacity (AP)	Classic: 4-5 devices BLE: 20 devices	8,000+ devices
Security	Classic: Fair BLE: Good	Exceptional
Energy efficiency	Classic: Fair BLE: High	High
RF penetration	Fair	Exceptional
Versatility	License-free and interoperable; Classic and BLE are not compatible with each other	License-free and interoperable
Data rates	Classic: 3 Mb/s BLE: 1 Mb/s BLE 5.0: 125 kb/s – 2 Mb/s	150 kb/s - 347 Mb/s

Morse Micro

Keeping Connectivity Secure

As an IEEE 802.11 Wi-Fi protocol, Wi-Fi HaLow follows globally recognized standards for secure IoT authentication and communication. HaLow supports the latest Wi-Fi requirements for authentication (WPA3) and AES encryption of over-the-air (OTA) traffic, with data rates that enable secure OTA firmware upgrades.

Although Bluetooth was originally "not intended to be a secure protocol" in and of itself, it has recently improved its security. For example, BLE now supports AES-CCM cryptography and 128-bit encryption. In addition, the Bluetooth Special Interest Group (SIG) continues to monitor and improve Bluetooth security features.

Energy Efficiency of Bluetooth and Wi-Fi HaLow

Wi-Fi HaLow was engineered to address the low-power requirements for a range of IoT applications, including sensor, audio, and video applications. It offers one of the most energy-efficient connectivity options, using only a fraction of the power of other versions of Wi-Fi.

Bluetooth Classic is primarily used for audio applications. It can transfer larger files, such as still images or low-rate videos, and is still relatively energy-efficient when compared to Wi-Fi 4, 5, or 6. BLE is more energy-efficient than Bluetooth Classic and designed for sensor applications and LE audio, consuming 10X less power than Wi-Fi 4, 5, or 6.

Versatility of Connectivity

Wi-Fi HaLow employs the unlicensed and class-licensed sub-1-GHz band, ranging from 850 to 950 MHz. Providing vendors achieve Wi-Fi Alliance certification for their Wi-Fi HaLow products, they will interoperate with other Wi-Fi HaLow-enabled products and networks.

It's worth noting that Wi-Fi HaLow and other Wi-Fi versions (Wi-Fi 4, 5, and 6) are all part of the IEEE 802.11 standard and operate on different RF bands, enabling them to coexist without impact to RF performance. This is a key advantage for networks designed to capitalize on Wi-Fi HaLow's unique benefits of long range, superior penetration, and energy efficiency.

Bluetooth similarly uses the unlicensed 2.4-GHz band; the Bluetooth SIG also offers certain qualifications. However, Bluetooth Classic and BLE aren't compatible, which means devices such as cell phones typically implement both versions to communicate with different end Bluetooth devices in the same band.

It's worth noting that Wi-Fi HaLow and other Wi-Fi versions (Wi-Fi 4, 5, and 6) are all part of the IEEE 802.11 standard and operate on different RF bands, enabling them to coexist without impact to RF performance.

Comparing Data Rates

Wi-Fi HaLow provides a range of data rates ideally suited for IoT devices, for example from 150 kb/s using MCS 10 with BPSK modulation, to a top rate of 4.4 Mb/s using MCS 9, with a single spatial stream at the narrowest bandwidth of 1 MHz. In an 8-MHz operating channel, a single-stream Wi-Fi HaLow AP can support a mix of IoT devices from very-low-power sensors, sending 1-MHz packets at rates down to 150 kb/s, to cameras sending 8-MHz packets at rates up to 43 Mb/s.

Bluetooth has much lower data throughput—just a fraction of Wi-Fi HaLow's top speed. Bluetooth Classic supports speeds up to 3 Mb/s, while BLE provides around 1 Mb/s (maximum 2 Mb/s if you're using Bluetooth 5).

Final Thoughts

While many consider Bluetooth Classic to be an indispensable protocol for today's wireless audio landscape, it doesn't provide a comprehensive solution for diverse long-reach, high-capacity, low-power IoT networks.

If your networking needs call for secure, power-efficient, and large-scale connectivity, Wi-Fi HaLow provides the optimal overall solution for the diverse requirements of your IoT networks. ■

References

1. https://www.wi-fi.org/discover-wi-fi/wi-fi-certified-halow

2. https://www.wi-fi.org/beacon/neil-weste/the-future-of-farming-testing-the-rural-range-of-wi-fi-certified-halow

3. https://www.silabs.com/documents/public/application-notes/an1137-bluetooth-mesh-network-performance.pdf

WEST·BOND's New 7KF

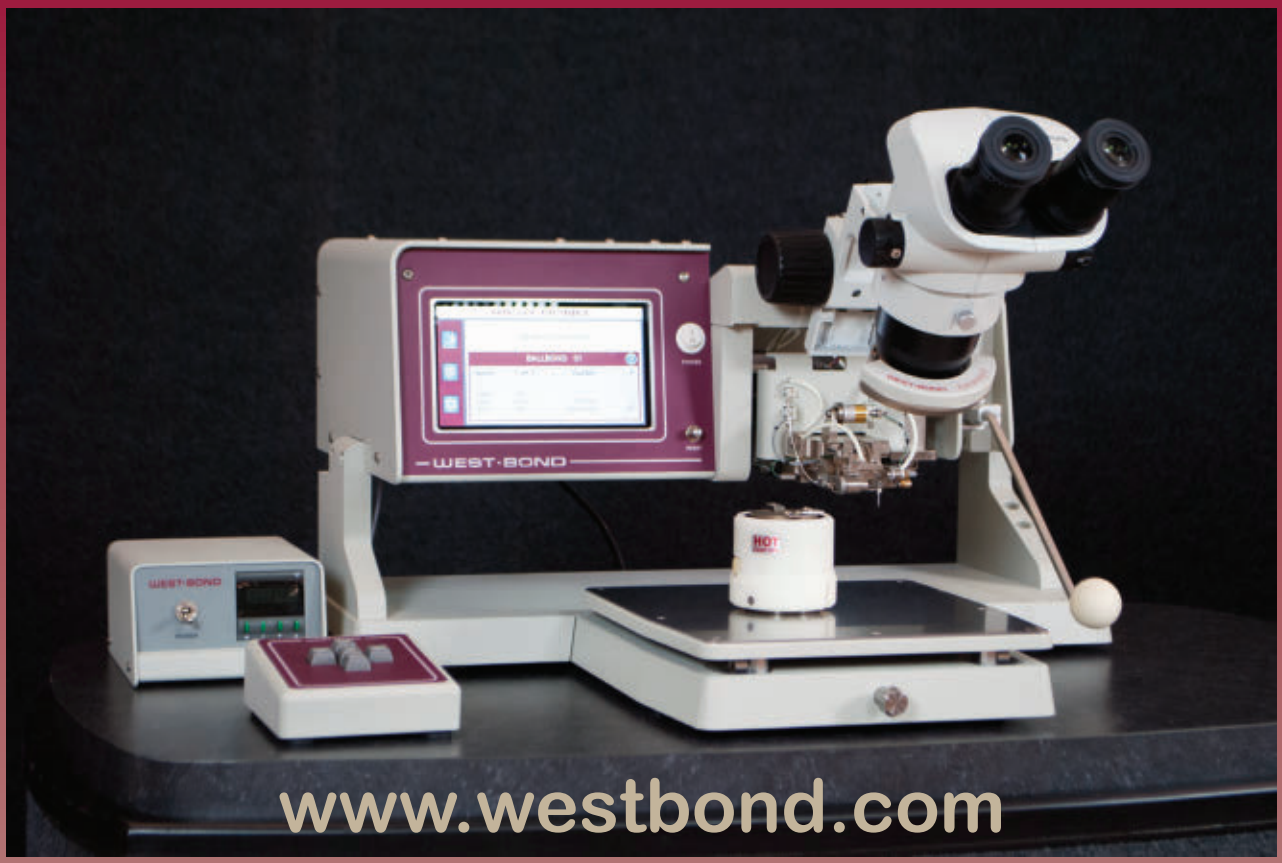

Helping you make that crucial connection since 1966

7KF Wedge-Wedge and Ball Wedge wire bonding system:

- 7" Capacitive Touch Screen
- Programmable Force and Tool Heat
- Primary and Secondary Ball Size Control
- Cu Ball Option Available
- Cortex M7 Microcontroller
- High and Low Frequency

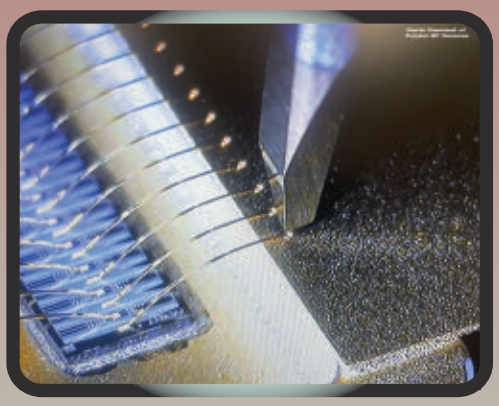

WEST·BOND®

1551 S. Harris Court Anaheim, CA 92806
Ph. (714) 978-1551
E-Mail: sales@westbond.com

Made In the U.S.A.

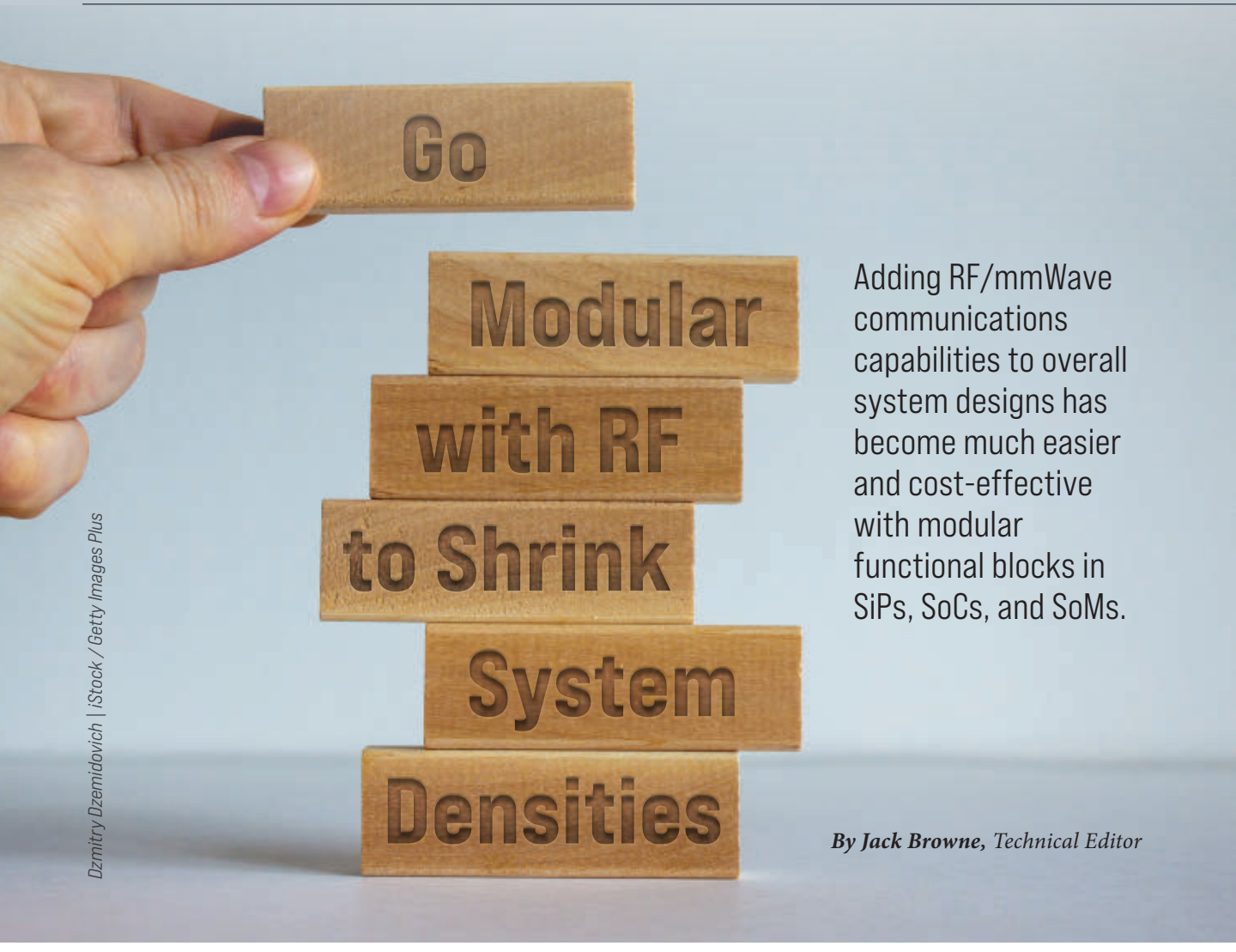

Dzmitry Dzemidovich | iStock / Getty Images Plus

Go Modular with RF to Shrink System Densities

Adding RF/mmWave communications capabilities to overall system designs has become much easier and cost-effective with modular functional blocks in SiPs, SoCs, and SoMs.

By Jack Browne, *Technical Editor*

Communications systems play major roles in the progress of humanity, enabling almost instant sharing of important messages. Beyond its human users, communications systems of the future are expected to have even more electronic and machine users, connected via the internet. Internet of things (IoT) sensors will provide instantaneous data for monitoring the environment, homes, and offices. Robotic assistants on land, sea, and in the air will make many lives easier.

Communications are important for maintaining the functionality and performance of all these devices. Thus, adding communications capability of some kind will be an important part of the design and development of many new electronic system designs.

Fortunately, communications systems and subsystems are becoming smaller and more integrated. This makes it easier to include them in electronic designs that meet military and aerospace reduced (SWaP) guidelines and are cost-effective for commercial and industrial users.

Drop-In Subsystems

Fielding a communications system once called for an array of components, such as mixers, amplifiers, and oscillators, connected as receivers, transmitters, or transceivers. Now, most of the components are in a single device, such as a system-in-package (SiP) or system-on-chip (SoC) small enough to fit within a single multi-pin package.

These drop-in subsystems are enabling the miniaturization of land-mobile radios and satellite communications (satcom) equipment. They also provide radio links for automobiles and even unmanned aerial vehicles (UAVs) with the addition of just a few components.

Such chip-sized radios ease the integration of embedded communications into many electronic products and offer multiple forms of communications, including data sharing between electronic devices. In slightly larger sizes, integrated modules with two or more ICs, even antennas, will support the expansion of 5G wireless networks and user equipment.

SiPs vs. SoCs

The distinction between SiPs and SoCs isn't always clear, although both are the end-results of efforts to miniaturize electronic products with greater numbers of functions. For higher-volume applications, when it's helpful to drop a complete system solution onto a circuit board, a SoC provides all of the components needed for a system with a minimal number of interconnections, usually to closely spaced package pins.

A SiP may more resemble a subsystem, with several SiPs connected to form a complete system. SiPs are better suited for design and development stages of a product, when it may be necessary to understand how different subsystems operate together under different operating conditions.

A SiP usually consists of several integrated circuits (ICs) with supporting passive circuit elements within the same chip carrier package. One example is a BGA package that can perform multiple functions of an electronic system, such as computing and communications. A SiP may contain RF receivers, transmitters, transceivers, a central processing unit (CPU), and computer memory on the same substrate.

In contrast, a SoC is a full system, such as a receiver, transmitter, or transceiver, with microcontroller or microprocessor and central processing unit (CPU), memory, and memory interfaces, contained within a package. When size isn't critical, larger solutions are available as system-on-modules (SoMs), with combinations of communications, computing, artificial intelligence (AI), digital signal processing (DSP), and even radar detection on a single printed circuit board (PCB).

A Look at SoCs and SiPs on the Market

For the level of integration possible, the ADRV9029 from Analog Devices is a SoC containing a frequency-agile transceiver for 75 to 6000 MHz in a 289-ball, chip-scale ball-grid-array (CSP_BGA) package measuring only 14 × 14 mm *(Fig. 1)*.

1. As an example of an SoC, this 75- to 6000-MHz agile transceiver is housed within a 289-ball, CSP_BGA package measuring 14 × 14 mm. Analog Devices

2. Though this is a larger SoC, coming in a 27- × 20-mm, 736-ball BGA housing, the transceiver has eight receivers and transmitters for 650 to 6000 MHz. Analog Devices

The compact housing holds four independently controlled transmitters and receivers, a pair of observation receivers for monitoring the transmitters, on-board frequency synthesizers, and DSP for a complete transceiver.

The ADRV9029 includes manual and automatic attenuation control and quadrature error correction (QEC), in the size of what was once a single device. But it's a good fit for wireless communications in 3G, 4G, and 5G wireless networks and in base stations with multiple-in, multiple-out (MIMO) antenna configurations.

The company offers several evaluation kits with PCBs to help understand how to use SoCs in its RadioVerse line, and have them occupy less circuit-board area without thermal or electromagnetic (EM) repercussions. In a larger, 27- × 20-mm, 736-ball BGA housing, the model ADRV9040 is a transceiver SoC for 650 to 6000 MHz with eight differential transmitters and eight receivers *(Fig. 2)*.

Analog Devices and Texas Instruments both developed strong assortments of SiPs in support of RF through millimeter-wave communications. While they may not provide the full functionality of an SoC, the SiPs integrate many necessary components and encourage high circuit density.

Analog Devices is paving the way to millimeter-wave (mmWave) communications in 5G wireless networks and other systems with a line of frequency converters in surface-mount-technology (SMT) packages operating as high as 86 GHz. For example, the ADMV7420 is a SiP in-phase/quadrature (I/Q) downconverter that translates signals from 81 to 86 GHz to an intermediate-frequency (IF) range of dc to 2 GHz.

The device is based on two function blocks: an input four-stage, GaAs low-noise amplifier (LNA) and a frequency downconverter. It consists of a GaAs in-phase/quadrature (I/Q) downconverter, on-chip buffer amplifier, and 6× frequency multiplier. The 6× multiplication is achieved with a cascade of 3× and 2× multipliers.

Most of the essential high-frequency components needed for downconversion of mmWave frequencies are packed into a 34-terminal, chip-array, small-outline, no-lead-cavity (LGA_CAV) housing measuring just 11 × 13 mm. The downconverter's mixer provides differential I and Q signals suitable for direct conversion.

A companion frequency upconverter, ADI's model ADMV7320, also relies on high-level integration to integrate numerous high-frequency components into a small package. It's based on three function blocks: a frequency mixer and local-oscillator (LO) path; envelope detector, variable-gain amplifier

(VGA), and power detector; and power amplifier (PA) and power detector. In a slightly larger 50-terminal, 16- × 14-mm LGA_CAV package, it achieves up to 33-dB conversion gain with minimum gain-control range of 40 dB. When set with 23.5-dB gain, it delivers +25-dBm typical output power.

Both frequency converters lack an on-board LO source, such as a frequency synthesizer, to form a full receiver or transmitter. They operate with a LO frequency range of 13.4 to 14.6 GHz but require additional LO. The ADMV7320 upconverter also has a built-in power detector and built-in envelope detector for LO nulling. Both are rated for operating temperature range of -40 to +70°C.

As important as the density that these devices bring to new communications equipment designs is the amount of evaluation they go through prior to final characterization. With proper interconnections to those multi-pin packages, users are assured of having a functional subsystem that will perform according to specifications, with a typical noise figure of 5 dB for both frequency converters.

Transceiver and Transmitter SiPs

Texas Instruments (TI), with one of the most agile and efficient websites in the industry, offers several RF SiPs with multiple transmitters and receivers for military and commercial radio applications. Model AFE7901 is a transceiver SiP that integrates a total of four RF sampling transmitter chains and four RF sampling receiver chains by means of eight digital-to-analog converters (DACs) and eight analog-to-digital converters (ADCs).

The AFE7901 operates from 5 MHz to 7.4 GHz in a flip-chip, ball-grid-array (FCBGA) package measuring 17 × 17 mm with 0.8-mm pitch. The DACs run at 12 Gsamples/s while the ADCs capture signals at 3 Gsamples/s.

With the aid of its digital upconverters (DUCs), the transceiver SiP can perform direct RF sampling at L-, S-, and C-band frequencies without frequency conversion, enabling light weight and miniaturization in portable radio systems. Digital step attenuators (DSAs) support amplitude tuning resolution of 0.125 dB over a 40-dB dynamic range for transmissions and 0.5 dB over a 25-dB dynamic range when receiving. The transmission bandwidth can be as wide as 400 MHz.

When even more bandwidth is needed, TI's model AFE8000 provides eight transmitters and 10 receivers with a transmission frequency range of 5 MHz to 7.125 GHz and receive range from 100 MHz to 7.125 GHz.

The transmitter is capable of eight channels at 800-MHz bandwidth or four channels each with 1.2-GHz bandwidth. Meanwhile, the receiver can be set for eight channels each with 800-MHz bandwidth or eight channels with 400-MHz bandwidth and two channels each with 800-MHz bandwidth. This transceiver also uses 12-Gsample/s DACs and 4-Gsample/s ADCs and comes in several configurations with different channel counts, all in a 17- × 17-mm FC-BGA package.

With these capabilities packed into such a small, low-power device, it's a good fit for radar and electronic-warfare (EW) systems as well as wireless communications in all markets. The SiP is scalable for various applications and provides fast switching speeds needed for time-division-duplex (TDD) communications systems.

For low-power radio applications, the models CC1110Fx and CC1111Fx are SoCs with MCUs, memory, USB controllers, and sub-1-GHz transceivers. Well-suited for automatic meter reading and low-power telemetry applications, these transceivers operate at the unlicensed bands at 315, 433, 868, and 933 MHz. The SoCs are supplied on a 36-lead chip carrier.

Automotive Modules

Mistral Solutions builds upon TI's creativity, basing its board-level mmWave radar kits and modules on TI's ICs. The 60- and 77-GHz automotive radar kits leverage the IWR6843 IC from TI to form complete frequency-modulated, continuous-wave (FMCW) radar modules available with two different antennas. Although large next to SiPs, they're complete automotive radars contained within enclosures measuring 54 × 53 × 18 mm and weighing just 15 g, with three transmit and four receive channels.

Also targeted at automotive applications, u-blox offers a variety of IoT communications modules, including automotive navigation modules based on its model UBX-M8030-Kx-DR 3D ADR GNSS IC. The modules combine GNSS navigation data with individual wheel speed, gyroscope, and accelerometer data for reliable navigation even when a vehicle changes speed.

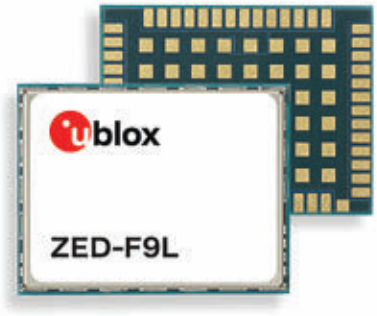

3. This navigation module is designed for use with GNSS L1 and L5 satellite signals in support of TCU and V2X automotive applications. u-blox

For example, model ZED-F9L is an L1 (1575.42 MHz) and L5 (1176 MHz) dual-frequency GNSS receiver module *(Fig. 3)* with 50-Hz update rate for low-latency navigation, telematics control unit (TCU), and vehicle-to-everything (V2X) communications applications. It helps drivers find a location even when satellite navigation signals are obstructed, such as through tunnels and indoor parking garages.

The three-dimensional automotive dead reckoning (3D ADR) provided by the module complements automotive navigation based on GPS and GNSS satellite navigation systems. It also contains anti-jamming and anti-spoofing hardware and software. In addition to the naviga-

Broadband RF power transistors, modules, and evaluation amplifiers: Polyfet RF Devices offers them all.

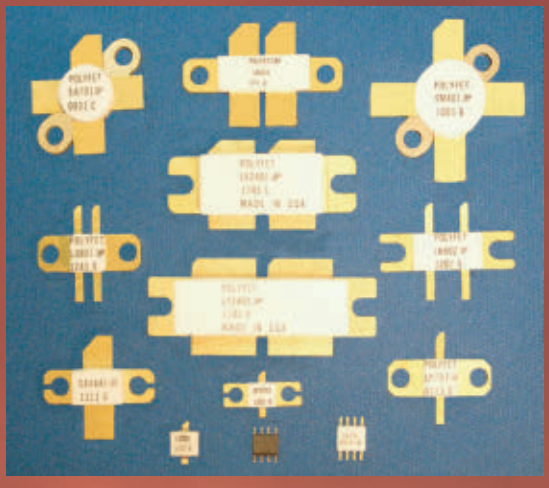

GaN: 28VDC and 48VDC, up to 3GHz, up to 160W, single-ended and push-pull.

LDMOS: 5-50VDC, up to 1.5GHz, up tp 2kW, single-ended and push-pull.

VDMOS: 12.5-50VDC, up to 1GHz, up to 400W, single-ended and push-pull.

Broadband RF power modules:
Utilize GaN and D-MOS technologies.
24-48VDC, up to 1260MHz, up to 350W CW,
various case sizes and RF connection types.
Custom design requests welcomed.

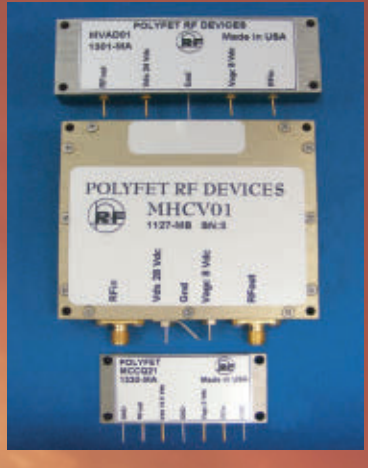

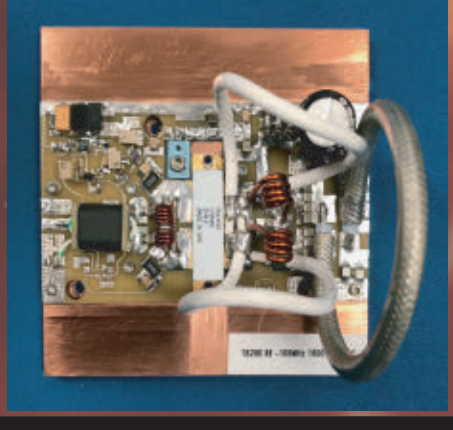

Various evaluation amplifiers available:
Displayed here is the TB280. It demonstrates the LY2542V (LDMOS) putting out 1kW, 22dB across 88-108MHz with 50VDC supply.

tion modules, u-blox also developed standalone wireless IoT modules with three radios in each: Wi-Fi 6, Bluetooth LE, and Thread.

WLAN, Wi-Fi, and FEM SoCs

Broadcom simplified the addition of IEEE 802.11 wireless local-area networking (WLAN) capability to electronic products with the development of WLAN SoCs based on its BCM4778 dual-frequency L1L5 GNSS receiver. The SoC receiver is designed to provide WLAN interconnections at low power levels with jamming protection and a full range of in-band and out-of-band filtering. By employing the company's Grid Tracking technology, it maintains wireless connections between parties even in settings with large numbers of users, such as densely populated urban environments.

By employing the company's Grid Tracking technology, it maintains wireless connections between parties even in settings with large numbers of users, such as densely populated urban environments.

Rather than a complete system, many SoCs provide key parts of the system, such as transmit/receive (T/R) front-end modules (FEMs) from Qorvo with both low-noise amplifiers (LNAs) and power amplifiers (PAs) in the package. Based on GaN semiconductor technology for the PAs and GaAs for the LNAs, the FEMs supply as much as 10-W output power from a 7- × 5-mm LGA housing.

The QPF5010 is the high-power member of the family, with 10-W output power from 8 to 12 GHz and power-added efficiency of 30% to 40%. Although in such small housings, they incorporate four blocks—a T/R switch, PA, LNA, and limiter.

Such FEMs ease the task of maintaining signal power in 5G or satcom infrastructure equipment, since the PAs and LNAs can be mounted physically close to the antennas to provide increased gain and power for transmission and reception, respectively.

MACOM Technology Solutions developed its model MAMF011099 5G antenna beamforming FEM to enhance Ka-band transmit and receive operations from 24.25 to 29.00 GHz. The module features three MMICs, which include a LNA, PA, directional coupler, and switch driver, to serve the signal path between a base station and antenna, all in a lead-free, 40-lead, 6.5- × 6.5-mm AQFN package. Both the PA and LNA are powered by +5 V dc.

Quectel Wireless Solutions, supplier of antennas and transceiver modules that are meant to boost signals from 4G/5G antennas, offers the FGH100M Wi-Fi HaLow module. It's for the sub-1-GHz version of Wi-Fi (IEEE 802.11ah) meant to provide much greater wireless communications range than traditional Wi-Fi radios for smart cities, smart buildings, and smart warehouses. It operates in the 850- to 950-MHz band with +21-dBm maximum output power and 32.5-Mb/s maximum transmission speed.

To help with wireless data flow around offices and homes, MaxLinear developed a line of Wi-Fi SoCs certified to Wi-Fi 6 and Wi-Fi 6E standards and housed in LFBGA packages measuring 12 × 17 mm. The SoCs can handle as many as four streams of 6-GHz data simultaneously.

Based on the company's WAV600 Series-2 Wi-Fi chipset, which operates to 4.8 Gb/s with higher-order modulation such as 1024 quadrature amplitude modulation (QAM), the SoCs can support as many as 256 users simultaneously, such as in a crowded office environment. The firm's AnyWAN broadband Wi-Fi SoCs are designed to provide wireless-area-network (WAN) service to hard-to-reach places.

Monitoring SoM

Qualcomm has applied its talents for integration to a line of robotics control and monitoring SoMs. The QRB2210 contains key analog and digital components for robotic control and monitoring under the roof of a single multi-pin package.

Well-suited for use in social assistants, education robots, at-home automated assistants, and surveillance systems, it's centered around a 64-bit Arm Cortex microprocessor capable of clock speeds to 2 GHz. It includes a DSP that's shared between the sensor core and audio subsystem as well as 720- × 1680-pixel display support. The SoM features Wi-Fi and Bluetooth connectivity for wireless remote control and communications.

SiP Service

For those seeking to develop custom SiPs, Teledyne e2v Semiconductors performs SiP packaging as a service. The company follows a customer's design requirements and, working with electrical and thermal simulations, they analyze the effects of different circuit layouts and density. Assembly is performed according to an agreed-upon strategy, followed by testing and product qualification.

All packaging assembly, testing, and screening is done according to industry standards, without issues from dealing with different component and material suppliers. In support of its SiP assistance, Teledyne e2v Semiconductors boasts AS9100 aerospace quality certification, multiple-zone baking ovens, and a Class 100 clean room. ■

RF Amplifiers and Sub-Assemblies for Every Application

Delivery from Stock to 2 Weeks ARO from the catalog or built to your specifications!

- Competitive Pricing & Fast Delivery
- Military Reliability & Qualification
- Various Options: Temperature Compensation, Input Limiter Protection, Detectors/TTL & More
- Unconditionally Stable (100% tested)

ISO 9001:2000 and AS9100B CERTIFIED

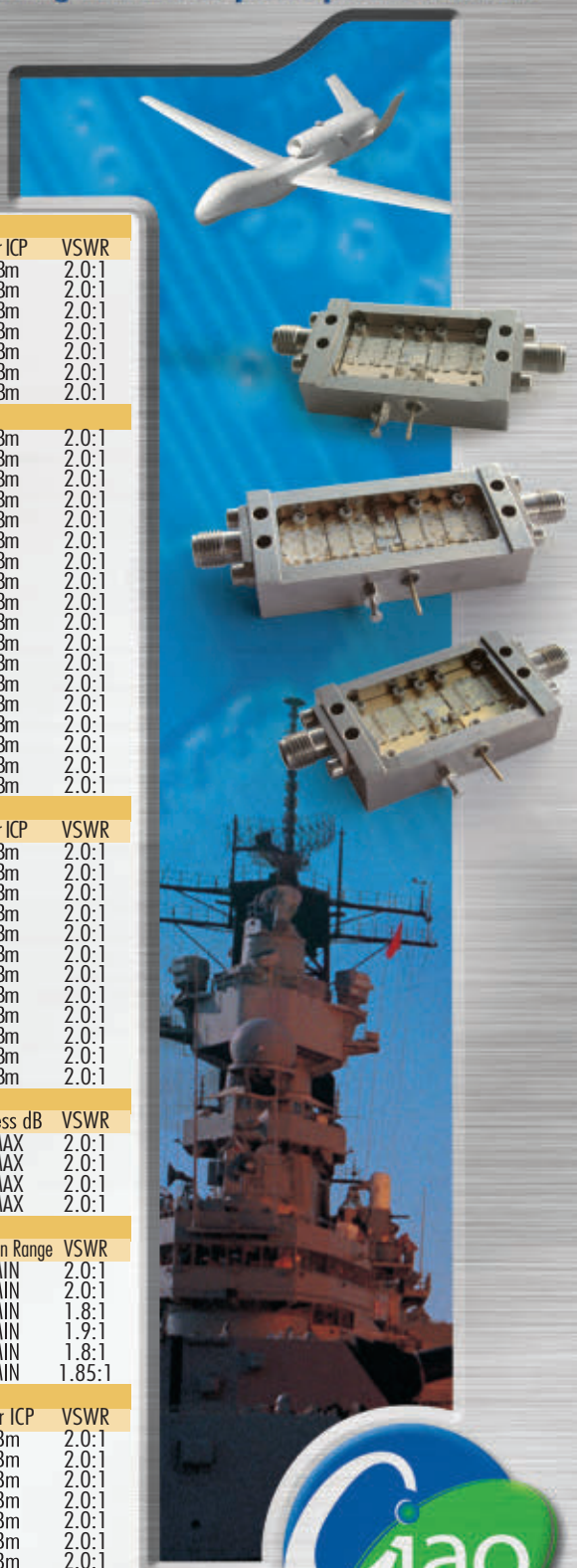

OCTAVE BAND LOW NOISE AMPLIFIERS

Model No.	Freq (GHz)	Gain (dB) MIN	Noise Figure (dB)	Power-out @ P1-dB	3rd Order ICP	VSWR
CA01-2110	0.5-1.0	28	1.0 MAX, 0.7 TYP	+10 MIN	+20 dBm	2.0:1
CA12-2110	1.0-2.0	30	1.0 MAX, 0.7 TYP	+10 MIN	+20 dBm	2.0:1
CA24-2111	2.0-4.0	29	1.1 MAX, 0.95 TYP	+10 MIN	+20 dBm	2.0:1
CA48-2111	4.0-8.0	29	1.3 MAX, 1.0 TYP	+10 MIN	+20 dBm	2.0:1
CA812-3111	8.0-12.0	27	1.6 MAX, 1.4 TYP	+10 MIN	+20 dBm	2.0:1
CA1218-4111	12.0-18.0	25	1.9 MAX, 1.7 TYP	+10 MIN	+20 dBm	2.0:1
CA1826-2110	18.0-26.5	32	3.0 MAX, 2.5 TYP	+10 MIN	+20 dBm	2.0:1

NARROW BAND LOW NOISE AND MEDIUM POWER AMPLIFIERS

Model No.	Freq (GHz)	Gain (dB) MIN	Noise Figure (dB)	Power-out @ P1-dB	3rd Order ICP	VSWR
CA01-2111	0.4 - 0.5	28	0.6 MAX, 0.4 TYP	+10 MIN	+20 dBm	2.0:1
CA01-2113	0.8 - 1.0	28	0.6 MAX, 0.4 TYP	+10 MIN	+20 dBm	2.0:1
CA12-3117	1.2 - 1.6	25	0.6 MAX, 0.4 TYP	+10 MIN	+20 dBm	2.0:1
CA23-3111	2.2 - 2.4	30	0.6 MAX, 0.45 TYP	+10 MIN	+20 dBm	2.0:1
CA23-3116	2.7 - 2.9	29	0.7 MAX, 0.5 TYP	+10 MIN	+20 dBm	2.0:1
CA34-2110	3.7 - 4.2	28	1.0 MAX, 0.5 TYP	+10 MIN	+20 dBm	2.0:1
CA56-3110	5.4 - 5.9	40	1.0 MAX, 0.5 TYP	+10 MIN	+20 dBm	2.0:1
CA78-4110	7.25 - 7.75	32	1.2 MAX, 1.0 TYP	+10 MIN	+20 dBm	2.0:1
CA910-3110	9.0 - 10.6	25	1.4 MAX, 1.2 TYP	+10 MIN	+20 dBm	2.0:1
CA1315-3110	13.75 - 15.4	25	1.6 MAX, 1.4 TYP	+10 MIN	+20 dBm	2.0:1
CA12-3114	1.35 - 1.85	30	4.0 MAX, 3.0 TYP	+33 MIN	+41 dBm	2.0:1
CA34-6116	3.1 - 3.5	40	4.5 MAX, 3.5 TYP	+35 MIN	+43 dBm	2.0:1
CA56-5114	5.9 - 6.4	30	5.0 MAX, 4.0 TYP	+30 MIN	+40 dBm	2.0:1
CA812-6115	8.0 - 12.0	30	4.5 MAX, 3.5 TYP	+30 MIN	+40 dBm	2.0:1
CA812-6116	8.0 - 12.0	30	5.0 MAX, 4.0 TYP	+33 MIN	+41 dBm	2.0:1
CA1213-7110	12.2 - 13.25	28	6.0 MAX, 5.5 TYP	+33 MIN	+42 dBm	2.0:1
CA1415-7110	14.0 - 15.0	30	5.0 MAX, 4.0 TYP	+30 MIN	+40 dBm	2.0:1
CA1722-4110	17.0 - 22.0	25	3.5 MAX, 2.8 TYP	+21 MIN	+31 dBm	2.0:1

ULTRA-BROADBAND & MULTI-OCTAVE BAND AMPLIFIERS

Model No.	Freq (GHz)	Gain (dB) MIN	Noise Figure (dB)	Power-out @ P1-dB	3rd Order ICP	VSWR
CA0102-3111	0.1-2.0	28	1.6 Max, 1.2 TYP	+10 MIN	+20 dBm	2.0:1
CA0106-3111	0.1-6.0	28	1.9 Max, 1.5 TYP	+10 MIN	+20 dBm	2.0:1
CA0108-3110	0.1-8.0	26	2.2 Max, 1.8 TYP	+10 MIN	+20 dBm	2.0:1
CA0108-4112	0.1-8.0	32	3.0 MAX, 1.8 TYP	+22 MIN	+32 dBm	2.0:1
CA02-3112	0.5-2.0	36	4.5 MAX, 2.5 TYP	+30 MIN	+40 dBm	2.0:1
CA26-3110	2.0-6.0	26	2.0 MAX, 1.5 TYP	+10 MIN	+20 dBm	2.0:1
CA26-4114	2.0-6.0	22	5.0 MAX, 3.5 TYP	+30 MIN	+40 dBm	2.0:1
CA618-4112	6.0-18.0	25	5.0 MAX, 3.5 TYP	+23 MIN	+33 dBm	2.0:1
CA618-6114	6.0-18.0	35	5.0 MAX, 3.5 TYP	+30 MIN	+40 dBm	2.0:1
CA218-4116	2.0-18.0	30	3.5 MAX, 2.8 TYP	+10 MIN	+20 dBm	2.0:1
CA218-4110	2.0-18.0	30	5.0 MAX, 3.5 TYP	+20 MIN	+30 dBm	2.0:1
CA218-4112	2.0-18.0	29	5.0 MAX, 3.5 TYP	+24 MIN	+34 dBm	2.0:1

LIMITING AMPLIFIERS

Model No.	Freq (GHz)	Input Dynamic Range	Output Power Range Psat	Power Flatness dB	VSWR
CLA24-4001	2.0 - 4.0	-28 to +10 dBm	+7 to +11 dBm	+/- 1.5 MAX	2.0:1
CLA26-8001	2.0 - 6.0	-50 to +20 dBm	+14 to +18 dBm	+/- 1.5 MAX	2.0:1
CLA712-5001	7.0 - 12.4	-21 to +10 dBm	+14 to +19 dBm	+/- 1.5 MAX	2.0:1
CLA618-1201	6.0 - 18.0	-50 to +20 dBm	+14 to +19 dBm	+/- 1.5 MAX	2.0:1

AMPLIFIERS WITH INTEGRATED GAIN ATTENUATION

Model No.	Freq (GHz)	Gain (dB) MIN	Noise Figure (dB)	Power-out @ P1-dB	Gain Attenuation Range	VSWR
CA001-2511A	0.025-0.150	21	5.0 MAX, 3.5 TYP	+12 MIN	30 dB MIN	2.0:1
CA05-3110A	0.5-5.5	23	2.5 MAX, 1.5 TYP	+18 MIN	20 dB MIN	2.0:1
CA56-3110A	5.85-6.425	28	2.5 MAX, 1.5 TYP	+16 MIN	22 dB MIN	1.8:1
CA612-4110A	6.0-12.0	24	2.5 MAX, 1.5 TYP	+12 MIN	15 dB MIN	1.9:1
CA1315-4110A	13.75-15.4	25	2.2 MAX, 1.6 TYP	+16 MIN	20 dB MIN	1.8:1
CA1518-4110A	15.0-18.0	30	3.0 MAX, 2.0 TYP	+18 MIN	20 dB MIN	1.85:1

LOW FREQUENCY AMPLIFIERS

Model No.	Freq (GHz)	Gain (dB) MIN	Noise Figure dB	Power-out @ P1-dB	3rd Order ICP	VSWR
CA001-2110	0.01-0.10	18	4.0 MAX, 2.2 TYP	+10 MIN	+20 dBm	2.0:1
CA001-2211	0.04-0.15	24	3.5 MAX, 2.2 TYP	+13 MIN	+23 dBm	2.0:1
CA001-2215	0.04-0.15	23	4.0 MAX, 2.2 TYP	+23 MIN	+33 dBm	2.0:1
CA001-3113	0.01-1.0	28	4.0 MAX, 2.8 TYP	+17 MIN	+27 dBm	2.0:1
CA002-3114	0.01-2.0	27	4.0 MAX, 2.8 TYP	+20 MIN	+30 dBm	2.0:1
CA003-3116	0.01-3.0	18	4.0 MAX, 2.8 TYP	+25 MIN	+35 dBm	2.0:1
CA004-3112	0.01-4.0	32	4.0 MAX, 2.8 TYP	+15 MIN	+25 dBm	2.0:1

CIAO Wireless can easily modify any of its standard models to meet your "exact" requirements at the Catalog Pricing.

Visit our web site at www.ciaowireless.com for our complete product offering.

Ciao Wireless, Inc. 4000 Via Pescador, Camarillo, CA 93012
Tel (805) 389-3224 Fax (805) 389-3629 sales@ciaowireless.com

MEMS vs. Crystal Oscillators:
It's All in the Application

Precision frequency control and timing are essential to all modern electronics technology.

By Ron Stephens, *Chief Operating Officer, Q-Tech Corporation*

Almost every electronic device you can imagine depends on a precision clock. Without precision oscillator clocks, all electronic communication would stop. This article compares the benefits of the latest precision clock technologies as they perform in different applications.

Introduced in the 1920s, the quartz crystal oscillator has long been the workhorse amongst electronic timing devices. A newer type of oscillator, which has been in development since the 1960s and available in production volumes since 2005, is the microelectromechanical-system (MEMS) resonator clock.

Today, MEMS oscillators have somewhat replaced crystal oscillators in many high-volume, low-cost applications. Like many things in the technology world, however, tradeoffs and exceptions must be considered depending on the application that's using the device.

Tradeoffs: MEMS vs. Crystal Oscillators

Figures 1a and *1b* show block diagrams of a MEMS oscillator and a crystal oscillator circuit. The MEMS oscillator is more complicated. In addition to a micromechanical silicon resonator, its digital circuitry includes a phase-locked loop (PLL) to determine and control frequency.

In comparison, the crystal oscillator is very simple and depends heavily on the very high "Q" quartz crystal resonator as the sole frequency-determining element shown in *Figure 1c*.

Both MEMS and crystal oscillators can be made more precise by using temperature compensation to achieve less than 1-ppm stability or oven-control to achieve parts-per-billion (PPB) levels of stability. In common parlance, crystal oscillators utilizing these compensation methods

are referred to as TCXOs and OCXOs, respectively. And while "XO" is specifically used for crystal oscillators, these terms are often used to refer to similarly compensated MEMS.

When it comes to absolute frequency stability over temperature, manufacturers are achieving great improvements in MEMS performance. SiTime, for example, is making MEMS that are almost arbitrarily precise by means of digital compensation techniques. It's important to understand the performance tradeoffs between quartz crystal oscillators and MEMS oscillators.

Phase Noise and Jitter

MEMS can withstand higher shock levels and are less susceptible to vibration sensitivity than quartz clocks. Since quartz resonators have a relatively larger mass, they also may experience fractures under very high shock levels.

Figure 2 compares phase noise for MEMS and quartz crystal oscillators. While MEMS can be made extremely precise in terms of stability and continue to improve in phase-noise and jitter performance, they can never be as good as quartz for static phase noise, jitter, and some other short-term stability parameters.

A benefit inherent to quartz crystal oscillators is their much higher "Q" level, which results in lower phase noise and lower jitter. Thus, in applications where this is important, quartz still reigns supreme. Also, the improved phase noise and jitter performance for MEMS always comes at the cost of even more power consumption.

Quartz oscillators are more efficient and reliable than MEMS devices whose complex circuitry consumes more power and can result in slower startup times. Moreover, quartz clocks can survive higher doses of radiation since MEMS clocks contain a non-radiation-tolerant PLL.

Temperature Stability

Figures 3 and *4* illustrate the reasons behind the most important tradeoffs between MEMS and quartz oscillators.

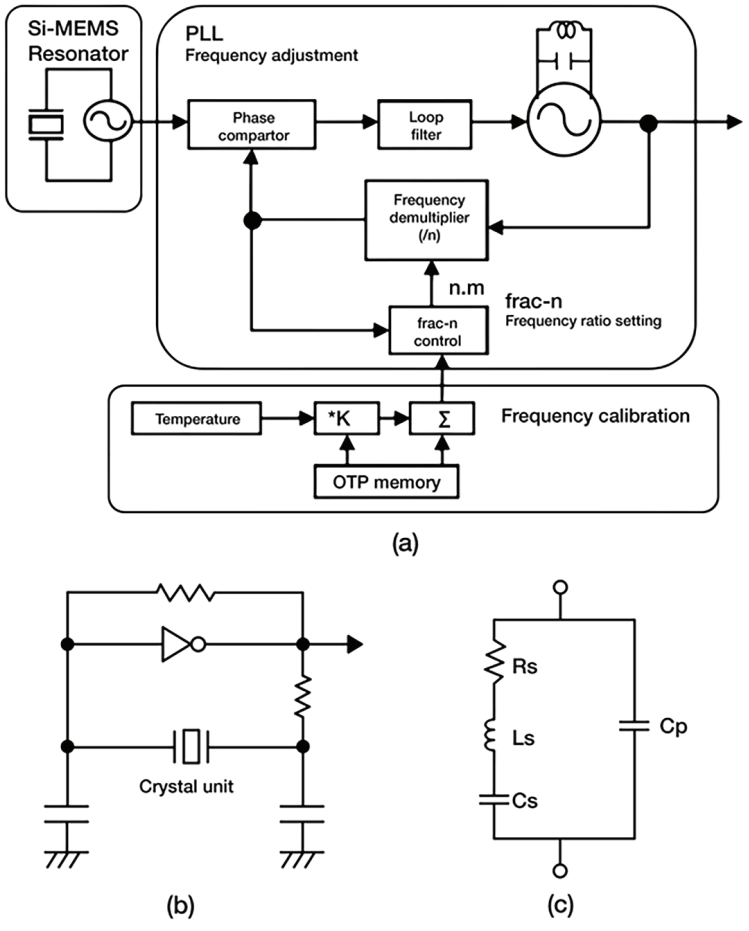

1. Block diagrams of the MEMS oscillator and the crystal oscillator circuit show the differences between the solutions. Images courtesy of Q-Tech

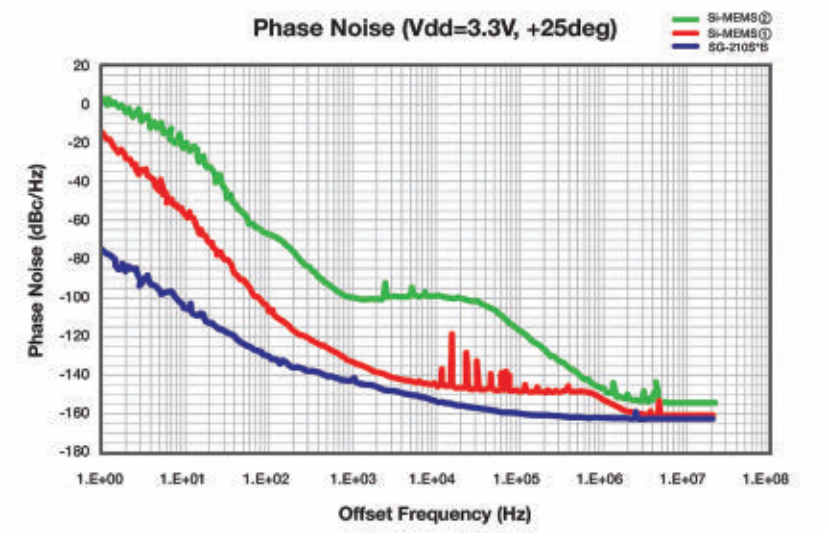

2. Phase-noise comparison of a quartz crystal oscillator vs. two equivalent MEMS oscillators.

Figure 3 shows the frequency vs. temperature performance of typical quartz oscillators compared to comparable MEMS devices. The first impression from this figure may be that MEMS oscillators actually demonstrate better frequency vs. temperature performance.

However, upon closer inspection, *Figure 4* reveals that, over time, the MEMS oscillators have frequency jumps whenever the division ratio switches to compensate for temperature changes. The high "Q" quartz crystal gives an inherently stable and smooth curve.

The MEMS resonator can be digitally corrected to be almost any level of stability. However, that comes at the cost of increasing power consumption.

The MEMS resonator can be digitally corrected to be almost any level of stability. However, that comes at the cost of increasing power consumption. Furthermore, it will always have micro frequency jumps over every short-term cycle that must be digitally corrected back to the desired level of stability.

The MEMS resonator curve isn't smooth, as it has a large number of small frequency jumps due to the dithering induced by digital correction. If more power is used, the dithering can be reduced, but never eliminated. This is what causes the MEMS clock to have worse phase noise and jitter than quartz crystal oscillators.

Manufacture and Cost

MEMS clocks offer several advantages over crystal oscillators in cost, production volume, and lead time. Because quartz crystal oscillators are inherently "custom," MEMS clocks are usually much cheaper and faster to produce.

Also, MEMS are manufactured in very high volumes using semiconductor manufacturing methods. Therefore, applications that don't need the good phase noise and the low jitter benefits of quartz, can tolerate the higher power consumption, and won't be exposed to any radiation, will often use the much less expensive MEMS.

Conclusion

Both technologies have their place in the future. On balance, MEMS oscillators already exhibit very good performance and represent an extremely valuable technological advance that will continue to be improved. They will dominate in high-volume low-cost clock applications, most notably in the automotive industry where low phase noise isn't important.

For their part, quartz crystal oscillators will continue to dominate space applications (where using MEMS isn't possible), as well as RF and microwave applications, radar, and other noise-sensitive circuits. ■

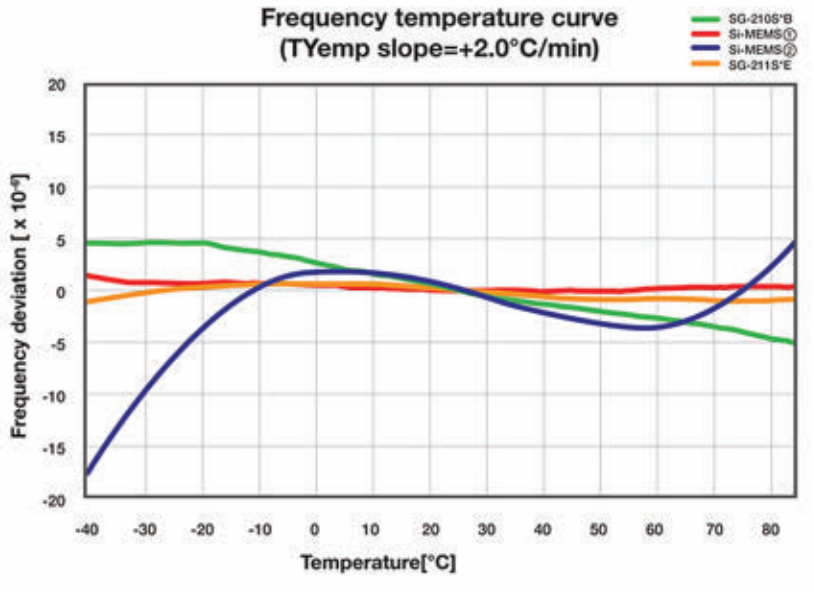

3. The graph compares frequency stability of quartz crystal vs. MEMS oscillators.

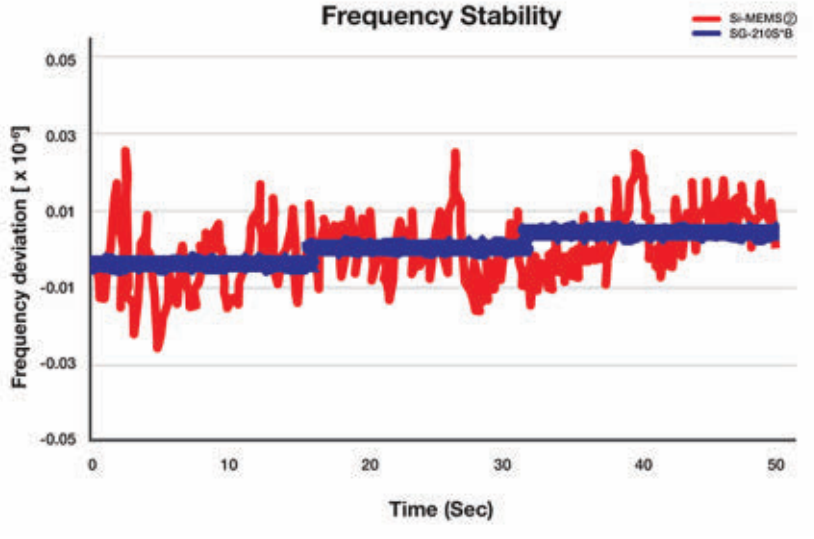

4. MEMS frequency stability exhibits frequency jumps unlike crystals.

Smart Wireless Multi-Sensor Module Offers ML Compatibility

TDK's InvenSense SmartBug 2.0 is an all-in-one wireless multi-sensor with updated functionality for consumer and IoT applications. It's available in two versions, a standard variety and a machine-learning version that can be used as a wireless data collector and/or tester with TDK machine-learning software. The switch between the two versions is made through a firmware update, and existing expansion boards with Wi-Fi, SD card, and ultrasonic sensor support will work with SmartBug 2.0.

TDK
https://tinyurl.com/2982y4qo

Signal Generator/Controller Programs 2,400 to 2,500 MHz

Mini-Circuits' model ISC-2425-25+ is a programmable signal generator and system controller for the 2,400- to 2,500-MHz industrial-scientific-medical (ISM) band. It tunes in 1-kHz frequency steps and provides output power from -30 to +25 dBm, adjustable with 0.01-dB resolution. Phase can be controlled in 1-deg. steps across a 360-deg. range. It's supplied in a compact metal enclosure measuring 3.86 × 3.15 × 1.57 in. (98 × 80 × 40 mm) with 50-Ω female SMA output connector and serial USB communications connector.

MINI-CIRCUITS
https://tinyurl.com/27y6ryhf

Amp Delivers 300 W from 2.4 to 2.5 GHz

Mini-Circuits' model ZHL-2425-250X+ is a solid-state power amplifier capable of as much as 300-W (+54.8 dBm) output power within the 2.4- to 2.5-GHz industrial-scientific-medical (ISM) band. Based on silicon LDMOS technology, the coaxial amplifier delivers 42-dB typical gain with 0.5-dB gain flatness and 60% power-added efficiency (PAE). It features built-in temperature monitoring and reverse-power protection, and an I^2C control interface, and provides regulated output power from 1 to 300 W for CW and pulsed signals at N-type and MCX connectors.

MINI-CIRCUITS
https://tinyurl.com/2zzeuq8s

Wireless Power Platform Delivers 600 W

Powermat Technologies' PMT350 600-W wireless power platform is based on the company's SmartInductive hybrid inductive/resonance technology. This latest 600-W platform is optimized for mid-power industrial, e-mobility, robotics, medical, and telecom applications. Powermat's wireless power technology is free from exact alignment or docking restrictions to make it more affordable to develop wirelessly powered systems with an optimized sub-$100 reference design ready for production. Able to significantly reduce OEM capital expenditures, the design includes full production files.

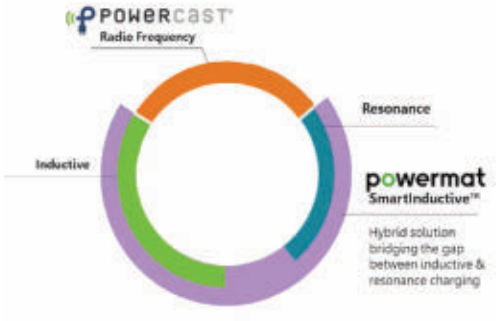

POWERMAT TECHNOLOGIES
https://tinyurl.com/29o92uma

Cost-Effective, Modular 2-Port VNAs Tout Performance, Ease-of-Use

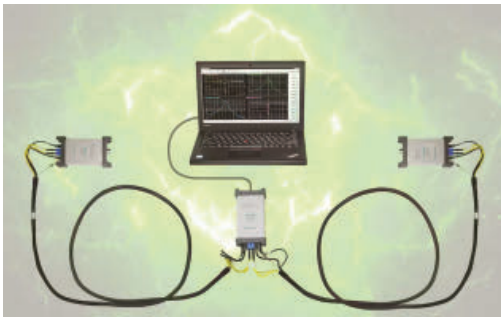

Anritsu's ShockLine ME7869A distributed, modular 2-port vector network analyzers (VNAs) can conduct long-distance, full-vector S-parameter measurements at distances up to 100 meters. Targeting existing and emerging commercial and military antenna design applications, three models are available, operating up to 8, 20, and 43.5 GHz, respectively. The ME7869A has two MS46131A 1-port VNAs that can connect directly to the antenna under test, and the cable length for each VNA module can be equal or different lengths, depending on the application.

ANRITSU
https://tinyurl.com/2bquc26j

Microwaves&RF

FUTURE DIRECTIONS FOR LPWANs AND THE IOT/IIOT

LEARN MORE IN OUR FREE ON DEMAND WEBINAR CREATED BY MICROWAVES & RF

LPWANs are the backbone that connects a multitude of battery-powered IoT/IIoT devices in applications such as asset tracking, occupancy detection, smart metering, and many others. There are several factors that wireless-network designers and integrators will want to consider as they sort through the various technologies available to them:

- What's the current state of the IoT/IIoT landscape? What is driving IoT adoption?
- How will LPWAN augment and work with other technologies like Wi-Fi and Bluetooth?
- What are some of the emerging applications for LPWANs?
- How will LPWANs address challenges of scalability?
- How will organizations like the LoRa Alliance continue making it easier to implement, develop, and deploy LPWANs?

REGISTER NOW AT:

http://www.mwrf.com/21265303

Speakers:

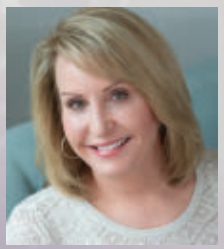

Donna Moore,
CEO and Chair of the LoRa Alliance

ENDEAVOR BUSINESS MEDIA